AMERICAN UNIVERSITY OF BEIRUT

DYNAMIC LTE NETWORK DIMENSIONING

by
MONA TAREK JABER

A thesis
submitted in partial fulfillment of the requirements
for the degree of Master of Engineering
to the Department of Electrical and Computer Engineering
of the Faculty of Engineering and Architecture
at the American University of Beirut

Beirut, Lebanon
May 2014

AMERICAN UNIVERSITY OF BEIRUT

DYNAMIC LTE NETWORK DIMENSIONING

by

MONA TAREK JABER

Approved by:

Prof. Zaher Dawy, Associate Professor — Advisor

Electrical and Computer Engineering

Prof. Youssef Nasser, Senior Lecturer — Member of Committee

Electrical and Computer Engineering

Prof. Joe Naoum-Sawaya, Assistant Professor — Member of Committee

Engineering Management Program

Date of thesis defense: May 7, 2014

AMERICAN UNIVERSITY OF BEIRUT

THESIS, DISSERTATION, PROJECT RELEASE FORM

Student Name: _____
Last First Middle

○ Master's Thesis ○ Master's Project ○ Doctoral Dissertation

☐ I authorize the American University of Beirut to: (a) reproduce hard or electronic copies of my thesis, dissertation, or project; (b) include such copies in the archives and digital repositories of the University; and (c) make freely available such copies to third parties for research or educational purposes.

☐ I authorize the American University of Beirut, **three years after the date of submitting my thesis, dissertation, or project,** to: (a) reproduce hard or electronic copies of it; (b) include such copies in the archives and digital repositories of the University; and (c) make freely available such copies to third parties for research or educational purposes.

_____
Signature Date

Acknowledgements

I would like to express my special appreciation and thanks to my advisor Professor Zaher Dawy, who has given me endless encouragement through my research and has allowed me to grow as a research engineer. I would also like to thank my committee members, professor Youssef Nasser and professor Joe Naoum-Sawaya, for serving as my committee members, for their insightful comments and hard questions thus motivating further my research and aim for excellence. Also, I would like to express sincere appreciation to Naeem Akl who has paved the way for my research by deriving essential statistical distributions.

An Abstract of the Thesis of

Mona Tarek Jaber for Master of Engineering
Major: Electrical and Computer Engineering

Title: Dynamic LTE Network Dimensioning

Radio network dimensioning is an essential step towards designing a cellular network and has traditionally relied on a pragmatic approach to capture the effects of fading and shadowing on the system interference. However, with the increased flexibility of LTE, which builds on the statistical variation of wireless channels by adapting resources accordingly, there is a need for new customized dynamic dimensioning methods. In this thesis, we develop the **S**tatistical **L**ink **B**udget **A**nalysis (**SLBA**) approach for LTE dimensioning that jointly accounts for fading and shadowing in the channel as well as loading due to traffic demand in the interference calculation. We utilize the derivation of the probability density functions (PDF) of four dimensioning parameters: SINR, noise rise, maximum allowed path loss and cell range in closed form. Results are generated and analysed to capture the LTE tradeoff between coverage, capacity, and quality constraints and the findings show tight dependency which invites a form of iterative process to optimise performance. Accordingly, an iterative algorithm that balances coverage and capacity requirements while respecting quality target is developed and implemented in a VBA/Matlab tool: **S**tatistical **A**nalysis of **LTE D**imensioning (**SALTED**). The algorithm is tested in a case study and results are benchmarked against traditional LTE dimensioning approaches with the help of a professional LTE network planning tool. The outcomes form this exercise show that the traditional approach leads to over-dimensioning at extra cost, thus, advocate the advantages of SALTED which yields dimensioning results comparable to those obtained with the professional planning tool.

Contents

List of Figures

List of Tables

Chapter 1

Introduction

Not many market analysts believed in the success of global system for mobile communication (GSM) or 2G when it was launched end of the second millennium. However, the demand of ubiquitous wireless coverage has taken an exponential growth since the GSM days and users have developed new taste for data services and less patience for delays and latency. Universal mobile telecommunications system (UMTS) or 3G was introduced at the start of the third millennium with the promise to provide the required capacity and quality. However, demand grew faster and more stringent than technology thus advances to basic 3G features were introduced resulting in high speed packet access (HSPA) or 3G+. The last addition to the cellular network family is the long term evolution (LTE), first released in 2008, which was hailed as the fourth generation but practically fits in the 3.9G category because it falls short of 4G requirements as defined by the 3GPP consortium. Since its introduction, LTE has been followed by advanced features thus forming LTE-Advanced and beyond. The main features of LTE include a flat IP-based network architecture, orthogonal frequency division multiple access (OFDMA)-based air interface, flexible bandwidth allocation (ranges between 1.4 MHz and 20 MHz), up to four times higher spectral efficiency than the state-of-the-art UMTS/HSPA cellular technology, low latency, and support for advanced multiple input multiple output (MIMO) techniques.

Similar to previous cellular generations, LTE requires proper radio network planning (RNP) to enable the claimed advantages of the technology. The RNP exercise takes a set of network requirements and constraints and finds the optimum sites' parameters and locations to meet the targets at minimum cost; thus it is a major milestone in the life and success of any network. Needless to say that the RNP process is highly complex and lengthy; consequently, it is typically divided into three main steps. The first consist of radio network dimensioning (RND) which takes pragmatic assumptions concerning user distribution and geographical areas distribution to facilitate the computation and lead to fast guidelines on inter-site distances and site parameters. The second step is the detailed planning

that includes as much information as is available to yield more realistic results pertinent to specific morphology mixes and user distributions. The third is an infinite process referred to as optimisation which deals with changing information and aims at adapting the network plan to accommodate them.

In this thesis, the prime focus is on the first step of RNP, where the hailed advanced features of LTE such as the adaptive modulation and coding scheme (MCS), MIMO, and flexible bandwidth, render the process of RND more complex and challenging than that of previous technologies. There are attempts to re-adapt UMTS and GSM dimensioning methodologies to LTE, however such an approach overlooks variations in key dimensioning parameters which would result in omitting intrinsic LTE gains that build on adapting to such variations.

LTE's MCS feature adapts to variations due to channel fading and shadowing and system interference, thus the system aims at allocating the suitable MCS to all users in view of current channel conditions, system conditions and user requirements. In traditional RND, this dynamic is ignored; instead, pragmatic margins are used usually looking at worst case scenarios and dimensioning accordingly. Besides, LTE's basic deployment relies on universal frequency planning, thus other users' and sites' activity on the shared frequency is bound to affect the noise level measured by a given user or site. This phenomena results in tight coupling between level of activity in the network and the actual achieved coverage. Again, this dependency is often omitted or pragmatically approximated in traditional RND methodologies which may lead to over or under dimensioning of the network.

Consequently, the gaol in this research is to develop an improved approach for LTE RND that is dynamic and sensitive to LTE flexible features. Such an RND approach cannot be deterministic nor one-directional, hence the steps towards developing it require revisiting RND concepts in the context of LTE and understanding incurred variations and dependencies.

The thesis objectives are the following:

1. Define LTE RND targets and constraints and derive a causal relation between key elements that would lead to designing the LTE link budget.

2. Integrate a statistical inter-cell interference approach in the link budget solution accounting for fading and shadowing on wanted and interfering signals.

3. Develop an iterative process, based on the statistical analysis, that captures the constraints dictated by coverage, capacity, and quality network design

targets and finds a balanced solution, i.e., inter-site distance and pertinent site parameters.

4. Develop an RND tool that incorporates the iterative RND process based on the statistical link budget analysis.

5. Benchmark results obtained from proposed RND process against traditional RND methodologies and compare to RNP results using a professional planning tool: Mentum Planet.

This report is organized as follows. Chapter 2 provides literature review and background information on topics of direct relevance to the thesis work. Chapter 3 presents the statistical approach to LTE link budget analysis (SLBA). The complete iterative process based on the statistical link budget analysis is presented in Chapter 4 as well as the corresponding tool implementation and functionality (SALTED). A case study is presented in Chapter 5 in which results from proposed RND are benchmarked against traditional RND through the use of professional RNP tool. Finally, Chapter 6 provides some concluding remarks and future research extensions.

Chapter 2

Literature Review

The objective of this literature survey is to give a general overview about some important concepts related to the thesis work. We start by giving description of radio network planning (RNP) with focus on the radio network dimensioning (RND) part. We then present the evolution of RND through cellular generations from 2G to 4G, followed by an overview of state of the art approaches adopted for LTE RND. These can be divided into three main categories: the traditional approach, the single sub-carrier statistical interference approach, and the multi sub-carrier statistical interference approach.

2.1 Radio network planning

Radio planning in general, is the process of selecting base station positions and corresponding parameters and optional features to provide sufficient coverage, capacity, and quality of service for the services required. The three objectives: coverage, capacity and quality of service in LTE are inter-dependent and interrelated hence they need to be addressed simultaneously.

Radio network dimensioning (RND) is the first level of the network planning process, which helps to conciliate the required coverage, capacity, and quality of service requirements in the network. Dimensioning is traditionally centered around the link budget analysis (LBA) which is basically a power budget balancing exercise that takes into consideration coverage, capacity and quality of service constraints. The outcome of the LBA is normally the maximum allowed path loss for each service. This is then used with a statistical propagation model (e.g., COST 231) appropriate for the area, to estimate the maximum cell coverage range, which is then used to estimate the required site density. The statistical propagation model however does not include terrain effects but often has a slope and intercept value for each type of environment otherwise referred to as clutter type (ex. urban, sub-urban, rural). Moreover, in the LBA phase users are as-

sumed uniformly distributed in the network such that each base station is equally loaded. This fairly simplistic approach allows nevertheless for a quick analysis and an indication of cell coverage range, subsequently site count requirements. The link budgeting also provides insight into the effects of different parameters and features on service coverage.

The second level of the radio planning process is traditionally performed using professional planning tools (ex Mentum Planet) to perform detailed predictions. In these tools, the propagation model takes into account the characteristics of the selected antenna, the terrain elevation, and the land use and land clutter surrounding each site. Also in these tools, an elaborate traffic modeling application is employed to represent realistically user's positions in the network and their different traffic profile. The second level in radio planning takes the output of the link budget analysis as starting point; at the end of the process the number of sites and locations would be optimised further. More detailed results are also obtained such as antenna azimuth and tilt, neighbouring and mobility parameter settings, and frequency planning where applicable. Radio network planning is an on-going activity in a live network. After the initial plan that resulted from the second level planning, the results will be continuously fine tuned with new inputs such a drive test data to adjust propagation model parameters, or updated live information on user distribution and service usage; this phase is often referred to as optimisation.

This thesis focuses on the RND part of the planning process which is the initial step in any network design but is also often revisited throughout the network life when more capacity is needed, or improved coverage or added features. Similarly, the first step in an RND exercise is the design of the LBA to capture the coverage, capacity and quality targets. An LBA built on analytical methodologies with no requirement for simulations presents a key advantage because of its ability to yield fast results. Accordingly it has been the norm in previous cellular generations to represent the effect of random variables such as fading and shadowing in the LBA through statistical margins, typically derived from simulation results compiled into lookup tables [2]. However, LTE's claim to increased spectral efficiency is based on the network's capability to adapt fast to signal to interference plus noise ratio (SINR) fluctuations. Moreover, LTE's flexibility in adaptive modulation and coding as well as multiple antenna techniques results in a myriad of possibilities hence an unmanageable number of entries in the lookup tables. Subsequently, the previously accepted detour is no longer suitable for LTE; therefore, there is a need to accurately capture the effect of fading, shadowing and loading in the LBA.

2.2 Evolution of radio network dimensioning

Traditionally, link budget analysis has been centered around Reudink's identified deterministic relationship between cell edge coverage provability and area coverage provability [3]. Cell edge reliability refers to the probability that the radio frequency (RF) signal strength measured on the contour at the cell edge will meet or exceed a desired quality threshold (e.g., -90 dBm). Whereas, cell area reliability is the probability that RF signal will meet or exceed the quality threshold after integrating the contour probability over the entire area of the cell. Because of this relationship, estimating the distance to the cell edge can be shown to be theoretically equivalent to determining the reliability of the signal strength within the cell. The effect of fading on cell range is depicted in Figure 2.1.

The received power at the cell edge can be expressed as in (2.2) and (2.3) where S

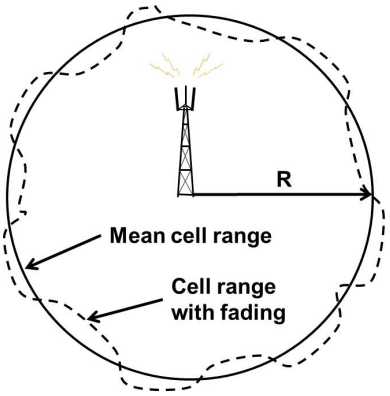

Figure 2.1: Effect of fading of cell range.

is the received power in dBm and Watt, respectively, T is the equivalent isotropic radiated power (EiRP) of the base station, L is the path gain (or loss), R is the cell range (km) from the base station, K and α are the propagation constant and propagation exponent, respectively, and δ_0 is the reference distance [4].

$$\begin{aligned} L &= 10^{K/10}\left(\frac{R}{\delta_0}\right)^{-\alpha} \\ L_{\mathrm{dB}} &= K - 10\cdot\alpha\cdot\log_{10}(R) + 10\cdot\alpha\cdot\log_{10}(\delta_0) \end{aligned} \tag{2.1}$$

$$\begin{aligned} S_{\mathrm{dBm}} &= T + L = T + K - 10\alpha\cdot\log_{10}(R) \\ S_{\mathrm{W}} &= T\cdot L = T\cdot 10^{K/10}\,(R)^{-\alpha} \end{aligned} \tag{2.2}$$

As presented in [1] a fading margin is used which results is cell radius reduction in order to guarantee a target coverage reliability as shown in Figure 2.2. The graph shows the received signal strength level (S_{dBm}) as a function of distance

away from base station. The mean path loss is shown by the dashed line and offset by the fade margin. The cell radius is defined in terms of the desired coverage reliability as the point where the solid line crosses the target quality threshold, S_τ.

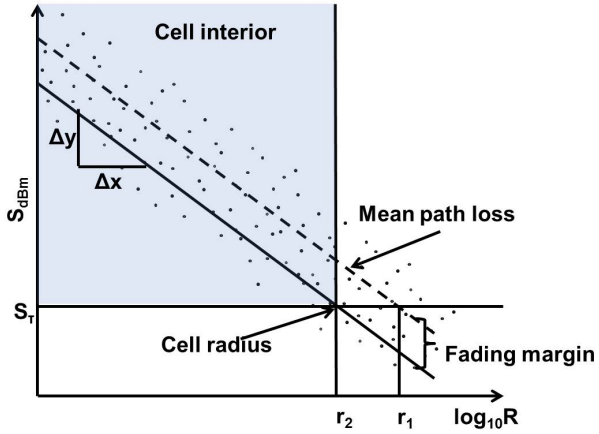

Figure 2.2: The mean cell radius is designated by r_1 and is determined by the crossing of the desired quality threshold S_τ. The mean cell radius is offset by a fading margin to guarantee a desired coverage reliability resulting in r_2. The ratio of Δ_y and Δ_x is equal to 10α, [1].

The received signal power as expressed in (2.2) represents only the mean power. However the received signal is not deterministic but is governed by both shadowing and fast fading. In Reudink's approach only shadowing is considered and is assumed to behave according to a zero mean normal random variable A with variance σ^2 (2.4). Thus, a more realistic representation of the received signal power is to express it as a random variable.

$$S = T + K - 10\alpha \cdot \log_{10}(R) + A \tag{2.3}$$

$$F_A(a) = 1 - Q(a) = \frac{1}{\sqrt{2\pi}} \int_{-\infty}^{a} e^{-\frac{x^2}{2}} dx \tag{2.4}$$

The edge coverage reliability can thus be expressed as in (2.5) where $F_A(a) = P(\xi \leq a)$ and $\xi \approx N(0, \sigma^2)$.

$$\begin{aligned} 1 - P_{out} &= P(T + K - 10\alpha \cdot \log_{10}(R) + A \geq S_\tau) \\ &= P(A \leq T + K - 10\alpha \cdot \log_{10}(R) - S_\tau) \\ &= F\left(\frac{T + K - 10\alpha \cdot \log_{10}(R) - S_\tau}{\sigma}\right) \\ &= 1 - Q\left(\frac{T + K - 10\alpha \cdot \log_{10}(R) - S_\tau}{\sigma}\right) \\ &= Q\left(\frac{S_\tau - T - K + 10\alpha \cdot \log_{10}(R)}{\sigma}\right) \end{aligned} \tag{2.5}$$

Traditionally, a fade margin, M_f is used to ensure the desired cell edge reliability, $F_A(a)$, which is approximated as $M_f = a\sigma$ (e.g., to ensure 75% cell edge reliability, a is the inverse of the normal function with probability 75%, mean set to zero and standard deviation 1 thus $a = 0.675$ and $M_f = 0.675 \cdot \sigma$). Thus it is possible to express the cell range R as a function of fading at any given target received power S_τ as follows:

$$R = 10^{\frac{T+K-S_\tau-M_F}{10\alpha}} \tag{2.6}$$

The area coverage reliability is then F_u and represents the fraction of usable area in the cell; it can be derived using Reudink's approach by integrating the contour reliability across the whole area:

$$F_u = \frac{1}{\pi \cdot R^2} \int_0^R (1 - P_{out}(r)) 2\pi r dr \tag{2.7}$$

The area reliability versus edge reliability relationship depends on two factors only: σ the fading standard deviation and α the path loss exponent (shown as B/10 in Figure 2.3).

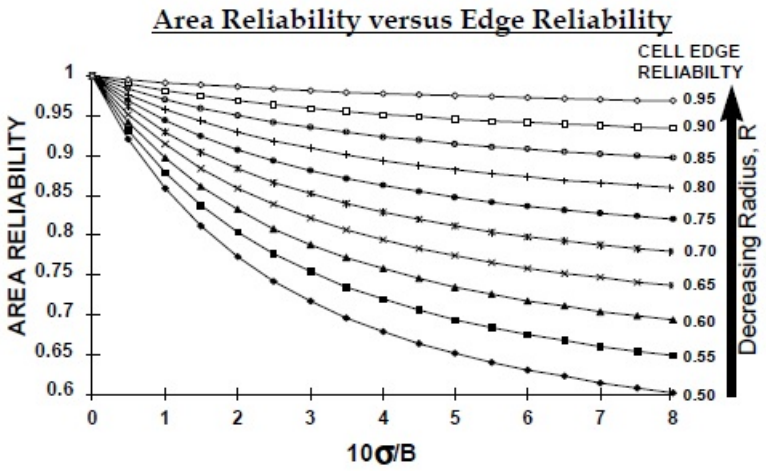

Figure 2.3: Area reliability versus edge reliability as a function of the ratio $\frac{\sigma}{\alpha}$. Note that α is shown as $B/10$ in the plot [1].

2.2.1 GSM link budget

The GSM standard was developed as a replacement for first generation (1G) analog cellular networks, and originally described as a digital, circuit-switched network. The launch of GSM took place in the latter part of 1992. Within seven years, GSM networks had over 50 million subscribers in Europe. By comparison, it took fixed networks nearly 50 years to acquire the same number of subscribers

worldwide, and about 15 years for the Internet to attract 50 million users worldwide [5]. The high demand in services and explosion in subscriber numbers necessitated the development of more spectrum efficient technologies such as 3G and 4G. GSM was not designed with spectrum efficiency as a prime objective, and was based on time division multiple access (TDMA) and frequency division multiple access (FDMA) access techniques. These techniques provide natural separation between the wanted signal and those of other users in the same cell and neighbouring cells. Ideally, TDMA separated users sharing the same frequency and FDMA separates simultaneous users; practically some leakage would happen between time slots and adjacent frequencies which should be accounted for. Consequently, GSM radio network dimensioning is focused on the signal to noise ratio (SNR) or simply the signal level at the cell edge (since the noise is basically thermal noise, a constant) using (2.6). A typical GSM downlink budget is shown in Table 2.1. Starting with the maximum power at the transmitter, the base station in the presented example, the effective isotropic radiated power (EiRP) is first calculated accounting for all gains and losses in the transmitter antenna chain. Then the receiver sensitivity is computed which represents the minimum signal perceived by the receiver and is calculated starting with the thermal noise power in the GSM channel, adding the receiver noise figure and the target SNR. The receiver noise figure is a none ideal realisation of any receiver whereby the receiver amplifier tends to amplify low signals (e.g., noise) more than high signals (e.g. required signal) which results in a hardware generated SNR degradation. More constraints are added to the receiver chain in order to account for power leakage between GSM time slots (interference in Table 2.1) and signal absorbtion due to the receiver proximity to the human body and the resulting antenna tilting. The receiver sensitivity with the two additional constraints constitute the GSM receiver gain. Additional design margins are added to account for channel fading and absorbtion loss upon the signal penetrating indoors. The final outcome of the link budget is the maximum allowed path loss (MAPL) which defines the maximum possible loss from propagation that can exist between receiver and transmitter in such a way that the transmitter is on full power and the receiver achieves the required SNR. Accordingly the MAPL is the difference between the EiRP and the total receiver gain affected by the design margins. From the third generation (UMTS) onward however, in the advent of quality oriented coverage and universal frequency planning, defining the target as a desired received signal at the cell edge becomes no longer adequate. A more suitable coverage target would be the SINR in which there are multiple random variables inter-playing, consisting of the wanted fading signal and the fading interfering signals from the neighbours.

Table 2.1: Typical GSM downlink link budget.

Parameter	**Unit**	**Formula**	**Value**
Transmitter power	W	a	20
	dBm	$b = 10 \cdot \log_{10}(1000a)$	43
TX antenna gain	dBi	c	18
TX cable loss	dB	d	-4
Combiner loss	dB	e	-4
Transmitter EiRP	**dBm**	$f = b + c + d + e$	**53**
Thermal noise density	dBW/Hz	h	-174
GSM channel bandwidth	KHz	i	270.833
RX noise figure	dB	j	8
Target SNR	dB	k	8
RX sensitivity	dBm	$l = h + 10\log(1000i) + j + k$	-103.7
Interference	dB	m	-3
RX body loss	dB	n	-2
Total receiver gain	**dB**	$o = l - m - n$	**-98.7**
Shadow fading margin	dB	p	8
Indoor penetration loss	dB	q	18
Total margin	**dB**	$r = q + p$	**26**
MAPL	**dB**	$s = f - o - r$	**125.7**

2.2.2 UMTS link budget

UMTS is based on spread spectrum modulation and is thus interference limited. Link budget dimensioning on the downlink is based on estimating the cell loading and corresponding required BS transmit power. Although performance in UMTS is typically measured in energy per bit to noise power spectral density ratio (E_b/N_o) the derivation here is provided as a function of SINR to ease comparison with other sections in the chapter. The relation between E_b/N_o and SINR is defined as below where W is the chip rate, a is the activity factor of the specific service, B is the bit rate corresponding to the service, S is the wanted received signal, N_t is the thermal noise, and I is the total interference:

$$\frac{E_b}{N_o} = \frac{W}{a \cdot B} \cdot \frac{S}{I + N_t}$$

On the downlink, UMTS uses orthogonal codes to separate users in the same cell. However, due to multipath propagation and resulting delay spread in the radio channel, orthogonality is partially lost at the receiver and the signal from the serving cell contributes partially to the interference level measured at the receiver. This additional interference is captured by the orthogonality factor, ω, which represents the effectiveness of downlink orthogonality (ω= 1: fully orthogonal in case of a single propagation path, typical values are between 0.4 and

0.6). Assuming there are U users in each cell and N neighbouring cells within measurable signal distances, SINR (γ_u) of user u can be expressed as follows:

$$\gamma_u = \frac{T_u \cdot L_{s,u}}{T \cdot L_{s,u}(1-\omega_u) + T\sum\limits_{n\neq s}^{N} L_{n,u} + \sigma^2} \tag{2.8}$$

Where T_u is the power required to serve user u and $L_{s,u}$ is the path loss between the serving cell s and user u. Solving (2.8) for T_u would lead to the following:

$$T_u = \gamma_u \left(T \cdot (1-\omega_u) + T\sum_{n\neq s}^{N} \frac{L_{n,u}}{L_{s,u}} + \frac{\sigma^2}{L_{s,u}} \right) \tag{2.9}$$

Summing up all the required transmit powers T_u to serve all users in cell s would result in the total cell power T as shown below, where the added factor a_u represents the activity factor of the given user; in other words, the percentage of time during which the cell needs to transmit to serve the given user:

$$\begin{aligned} T &= \sum_{u=1}^{U} a_i \cdot T_u \\ &= a_u \cdot T \cdot \gamma_u \sum_{u=1}^{U} \left((1-\omega_u) + \sum_{n\neq s}^{N} \frac{L_{n,u}}{L_{s,u}} \right) + \sigma^2 \sum_{u=1}^{U} (a_u \cdot \gamma_u \cdot (1/L_{s,u})) \\ &= \frac{\sigma^2 \sum_{u=1}^{U} \gamma_u \cdot a_u \cdot (1/L_{s,u})}{1 - \sum_{u=1}^{I} \gamma_u \cdot a_u \left((1-\omega_u) + \sum\limits_{n\neq s}^{U} \frac{L_{n,u}}{L_{s,u}} \right)} \end{aligned} \tag{2.10}$$

In a spread spectrum system, the ratio of other cell to own cell interference ratio is defined as the f-factor and depends on the path loss between the serving cell and the user ($L_{s,u}$) as well as all interfering neighbouring cells and the user ($L_{n,u}$), thus differs per user location:

$$f_u = \sum_{n\neq s}^{N} \frac{L_{n,u}}{L_{s,u}} \tag{2.11}$$

Accordingly, the downlink cell load is defined as η as follows:

$$\eta = \sum_{u=1}^{U} (\gamma_u \cdot a_u(1-\omega_u) + f_u) \tag{2.12}$$

Thus, equation (2.10) can be interpreted as "the total power in downlink is equal to the transmission power which would be needed in the absence of interference plus noise rise due to multiple access interference, which is in decibels

$\mu = -10\log(1-\eta)$" [6].

Consequently, downlink UMTS capacity outage probability is the probability of the required cell power exceeding the maximum effective isotropic radiated power (EiRP); which is the aggregate power determined by the maximum power amplifier and antenna gain chain. The randomness of the required power is due to the fading on the serving cell and the interfering cells as well, resulting in a scenario-specific required power distribution. Typically, monte carlo simulations are conducted to find the distribution of the f-factor, an acceptable value is deduced, which is used in (2.10). In addition, the randomness of the wanted signal in the numerator of (2.10) has been typically accounted for through log-normal fading margins as in Section 2.2 (which often include soft handover gain) and fixed power headroom to account for fast power control adaptation. These margins, in addition to the noise rise μ are also included in the coverage analysis based on the link budget thus capturing the spread spectrum cell breathing effect; an example DL UMTS budget is shown in Table2.2.

Firstly, the EiRP is computed based on the maximum transmit power, attenuated by the connecting cable chain, and amplified by the transmit antenna; similar to the GSM link budget. The receiver sensitivity is also similar to GSM with two major differences: cell load based interference margin and information rate gain. In UMTS the interference from other cells is due to the fact that all cells are continuously sharing the spectrum thus the level of interference is tied to the level of activity in neighbouring interfering cells as demonstrated earlier. On the other hand, the spread spectrum modulation results in a technology inferred gain referred to and processing gain or information rate gain. Low data rates that spread over a large channel benefit from higher processing gains than high data rates. Accordingly the receiver sensitivity in UMTS depends on the cell load but also differs among users nit he same cell, measuring the same interference, but using different data rates in their connections. The same design margins considered int he GSM link budget are reused for UMTS to account for shadowing effect and penetration losses. However two new margins become relevant with UMTS technology: soft hand over gain (or macro diversity gain) and power headroom. UMTS technology allows for users around cell borders to be connecting to more than one cell at the same time thus providing a form of spatial diversity, the resulting gain is either added int he link budget as a stand alone margin or a common margin that represents both shadowing and macro diversity is computed. Furthermore, UMTS relies on very fast power control algorithm to allow communication without the risk of jamming from a loud user. For this reason, a power headroom needs to remain on reserve to compensate for fast signal drops due to fast fading, a typical value is 2dB. On the other hand, body loss is not considered in the example UMTS link budget below since it is designed for data connectivity; body loss is mostly relevant for voice connections.

Table 2.2: Example of a UMTS downlink budget assuming 64kbps data rate and 50% cell load.

Parameter	**Unit**	**Formula**	**Value**
Data rate	kbps	a	64
Transmit power	dBm	b	33
Cable/connector/combiner losses	dBm	c	3
TX antenna gain	dBi	d	17
EiRP	dBm	$e = b - c + d$	47
Thermal noise density	dBm/Hz	f	-174
Receiver noise figure	dB	g	7.00
Cell load	**%**	η	**50.00**
Interference margin	**dB**	$\mu = -10\log(1-\eta)$	**3**
Receiver noise power	dBm	$i = f + g + \mu$	-163.99
Information rate	dB-Hz	$j = 10\log(1000 \cdot a)$	48.06
Minimum E_b/N_o required	dB	k	4.2
Receiver sensitivity	dBm	$m = i + j + k$	-120.13
Shadowing (log-normal) margin	dB	p	8
Soft handover gain (macro-diversity)	dB	q	3
Indoor penetration loss	dB	r	18
Power head room	dB	s	2
MAPL	**dB**	$L_m = e - m - p + q - r - s$	**142.73**

2.3 LTE radio network dimensioning

There are few papers dealing with analytical RND approaches for orthogonal frequency-division multiple access (OFDMA) technologies that can be grouped into three categories. The first group readopts the traditional dimensioning approach of 2G and 3G networks on LTE such as [7–10] (Section 2.3.1). Another group is the single sub-carrier group which represents a line of research that models the system interference considering a single sub-carrier scenario (Section 2.3.2). A third group of research is based on a statistical interference model with multiple sub-carrier considerations (Section 2.3.3).

2.3.1 Traditional LTE dimensioning

A typical downlink budget is presented in Table 2.3 where parameters have been grouped into those that are considered constants, and those that are considered random variables. The EiRP is defined the same way as previous technologies

(GSM and UMTS), it is however distributed equally over the number of available sub-carriers resulting in EiRP per sub-carrier (P). Other pertinent parameters to the receiver chain are mostly similar as well such as the thermal noise (measured over the sub-carrier width), the receiver noise figure, penetration loss and target SINR. Since all these parameters can be assumes deterministic, their aggregate effect is computed to determine the effective power per subcarrier (T). Two essential design margins, present in GSM and UMTS link budgets, remain unaccounted for: the shadowing margin and the interference degradation margin. These are shown in the variable parameters section of the link budget and are given special attention in the designing of the link budget as will be discussed in coming paragraphs. In order to simplify the representation, the effective power T

Table 2.3: Typical LTE downlink budget.

Constant parameters	**Unit**	**Formula**	**Value**
Total transmit power	dBm	P'	46
TX antenna gain	dBi	G_T	18
Cable/connector/combiner losses	dB	l	2.5
EiRP	dBm	$d = P' + G_T - l$	61.5
Total number of sub-carriers	10MHz	H	600
EiRP per sub-carrier	dBm	$P = 10 \cdot \log(\frac{10^{\frac{d}{10}}}{H})$	33.7
Thermal noise density	dBm/Hz	f	-173.8
Bandwidth per sub-carrier	Hz	W	15000
Total thermal noise in channel	dBm	$\sigma^2 = f + 10 \cdot \log(W)$	-132.0
RX antenna gain	dBi	G_1	0
RX noise figure	dB	L_1	7
Required SINR	dB	γ_τ	-2.1
Penetration loss	dB	L_2	18
Total gains	dB	$M_G = G_1$	0
Total losses	dB	$M_L = L_1 + L_2$	25
Effective power per subcarrier	dB	$T = P + M_G - M_L$	8.7
Variable parameters	**Unit**	**Formula**	**Value**
Shadowing margin	dB	M_f	8.5
Interference degradation margin	dB	M_μ	3

per subcarrier will be calculated based on the EiRP per subcarrier (P) by adding all deterministic gains and subtracting all deterministic losses as $T = P + M_G - M_L$ and is used in (3.4). In decibels, the maximum allowed path loss can be expressed as below which matches the link budget in Table 2.3:

$$\begin{aligned} 10 \cdot \log(L_m) &= K - 10\alpha \log(R) \\ &= 10 \log(\gamma_\tau) + 10 \log(\sigma^2) - 10 \log(T) + M_f + M_\mu \end{aligned} \quad (2.13)$$

Traditionally, M_f is derived assuming that the random variable A_s follows a log-normal distribution with an area specific shadowing standard deviation to guarantee a defined outage probability as in (2.4). The interference degradation margin M_μ, is often predefined irrelevant of the actual cell load such as in [7] and [10]. Consequently the cell range can be derived as follows:

$$R = 10^{\frac{10\log(\gamma_\tau)+10\log(\sigma^2)-10\log(T)+M_f+M_\mu-K}{10\alpha}} \tag{2.14}$$

Effectively, the traditional approach aims at finding the appropriate design margins that would guarantee a desired outage probability as depicted in Figure 2.4. The shadowing margin moves the cell range from the mean value depicted by the dashed line to a smaller value determined by the number of received signal instances that fall on the upper side of the bold black line. Once the percentage of received signal instances above the line is equal to the minimum required edge coverage probability, a suitable shadowing margin has been reached. In other words the shadowing margin results in a cell range margin that typically reduces the cell range to improve coverage probability. It is widely accepted in the cellar design field to approximate shadowing variations with a log-normal distribution. there are many simulations and remeasurements that have validated this assumption thus allowing the definition of a suitable shadowing margin without the need of simulations.

In addition to the shadowing margin, we should also account for the interference degradation margin. This impacts the target received signal power (S_τ), thus with higher interference levels from neighbouring cells, S_τ becomes more stringent. In Figure 2.4, S_{τ_1} represents the target received signal power for an isolated cell and S_{τ_2} represents the same in a real deployment scenario. Again, the cell range has been decreased by another margin determined by the interference degradation margin to account for interference coming from neighbouring cells. However, the simulations in Figure 2.4 do not help in determining the proper interference margin; for that one needs to conduct received SINR simulations and not received signal simulations. Moreover, the distribution of the resulting SINR is unknown at this stage, but it has been demonstrated that it is a factor of cell loading and fading conditions on each of the active cells in the network cluster.

2.3.2 Single-subcarrier LTE dimensioning

The single sub-carrier group represents a line of research that models the system interference considering a single sub-carrier scenario. For example, Seol et. al in [11] and [12] propose an elaborate derivation of inter cell interference (ICI) PDF under multipath Rayleigh and Ricean fading respectively, conditioned on the shadowing and the network load. Their objective is to point out the inaccuracy of assuming Gaussian ICI and its effect on transmitter and receiver design

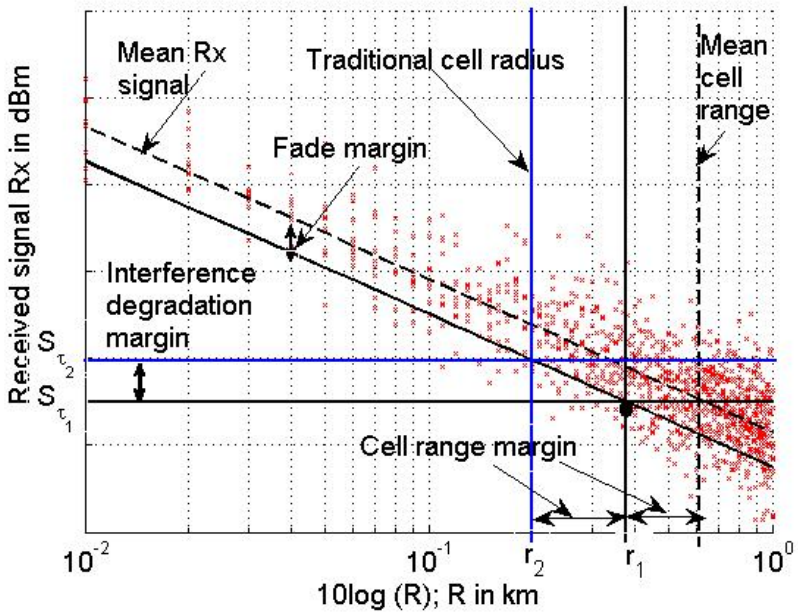

Figure 2.4: Cell range definition in the traditional link budget analysis as a function of fading margin.

in OFDMA. The approach is complex and relies on monte carlo simulations to derive averages, hence not suitable for dimensioning purposes. On the other hand, Ben Cheick et. al in [13] propose an outage probability analysis based on the statistical modeling of the downlink interference using two approaches: the Fenton-Wilkinson and the central limit theorem. They reach mathematically manageable equations but in the process, approximate fast fading effect of interfering cells' channels to their average value and consider full cell load. Yang and Fapojuwo in [14] propose an analytical framework for a hexagonal cellular network with Rayleigh fading only and consequently derive corresponding coverage probability and the spectrum efficiency characterisation. Perhaps the closest research line towards LTE dimensioning assuming single sub-carrier is that presented by Tabassum et. al in [15]. The authors capture accurately the effect of composite fading on the channels from the serving cell and interfering cells, while accounting for the scheduling algorithm impact on ICI. In order to reach an analytically tractable model for ICI, the authors divide each cell into K concentric circular regions in such a way that the path loss decay within each circular region remains constant or uniform. The analysis provides estimations of the outage probability and the cell ergodic capacity but does not proceed to use the outcome for dimensioning purposes. Moreover, the approach presented is semi analytical though and requires a heavy computational load which is not suitable for dimensioning purposes. Besides, the proposed approach captures advanced

features such as scheduling algorithms that are essential for feature evaluation and assessment however increase the complexity of the ICI modeling for the purpose of dimensioning.

2.3.3 Multi-carrier LTE dimensioning

Third group of research is based on a statistical interference model with multiple sub-carrier considerations. The single sub-carrier approach relies on an average SNR or SINR; however averaging the SINR on different tones which undergo different amounts of fading does not give an accurate representation of the channel. Standardisation WiMAX efforts [16] define a physical abstraction approach to map link layer performance indicator and channel quality indicator for different modulation and coding schemes. Channel quality indicator are derived from instantaneous channel state, such as the instantaneous SINR for each sub-carrier in OFDM. The two mostly used channel quality indicators in LTE are the exponential effective SINR and the mean instantaneous capacity. Link layer performance indicator is often the bit error rate but could also be packet error rate or symbol error rate.

Guiliano and Mazenga in [17] base their approach on the exponential effective SINR model as in [18] and [16] approximated by a Gaussian random variable. The approach however is complex and still relies on simulations while it ignores the effect of shadowing of interfering signals on the effective SINR. Kelif et. al in [19] propose an approach based on the mean instantaneous capacity concept as in [16] using the Fenton-Wilkinson method to approximate the joint effect of shadowing and fading on the SINR distribution but with similar assumptions as in [13] thus assuming full cell load.

It should be highlighted at this stage that neither the single nor the multi sub-carrier statistical interference studies have been actually developed into a complete dimensioning approach. The mathematical complexity of the multi-subcarrier statistical analysis in its current form conflicts with the essential requirement of RND being purely analytical and fast in providing results. It is anticipated at this stage that the single sub-carrier statistical interference analysis is more suitable for the RND specific application. It should also be re-emphasised that RND is a pre-planning step and is fundamentally based on simplified assumptions. Accordingly, compared to other universally accepted approximations such as flat area, the impact of replacing the multi-subcarrier consideration by single-subcarrier is esteemed to have lesser impact and hence may be suitable for RND.

Chapter 3

Statistical Link Budget Analysis Approach for LTE Cellular Network Dimensioning

As discussed in Chapter 2, the current RND approach for LTE networks is based on the traditional LBA but lacks information on interference distribution. This is often compensated for by pragmatic margins or simulations. Theoretically, the third line of research, referred to as the multi sub-carrier group, should lead to the ideal RND approach since it incorporates more details and variations pertinent to dimensioning. However, due to its complexity it often requires heavy computational load and simulations which renders this approach unsuitable for RND. Practically, the second line of research, referred to as the single-subcarrier group, is a better candidate since it allows manageable and purely analytical RND methodology. In the framework of RND, pragmatic assumptions that are not realistic are presumed by definition such as subscriber distribution and homogeneity of geographical area among others. It can be argued that single sub-carrier consideration is another pragmatic assumption added to the set of conditions of LTE RND since it enables the exercise to remain analytical and fast. Consequently, the approach developed in this thesis is based on ICI characteristics of a single OFDMA subcarrier on the downlink and aims at capturing tradeoffs between different dimensioning constraints. We first start by revisiting LBA concepts in the context of LTE to enable further development of the dimensioning approach.

3.1 LTE link budget factors

The system model assumes N three-sectored sites where each sector is modeled as a hexagon of diameter R and the base station is located at the intersection of the three sectors as shown in Figure 3.1. The cell edge user receives the required signal from the serving cell but also interference from the 20 other sectors in the

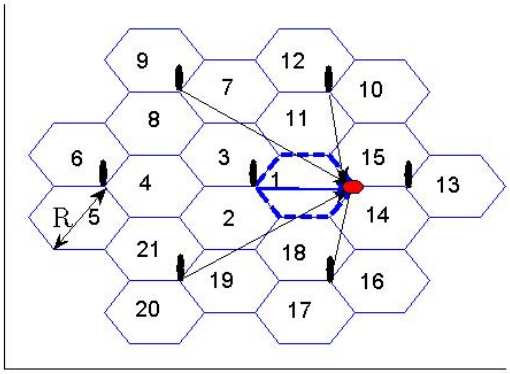

Figure 3.1: System model.

network. The inter-site distance is $3r/2$. Neighbouring cells have a cell load η_n which is the percentage of the used resources (power or sub-carriers) in the cell and should reflect the effective capacity demand from the subscribers covered by the given sector. For example if the maximum capacity of a sector is 35 Mbps and, on average, a subscriber consumes 50 kbps during the busy hour traffic, then the maximum cell capacity is 700 subscribers. Consequently, at 50% cell load, 350 subscribers can be adequately covered and the actual downlink throughput of the cell would be 17.5 Mbps; it would thus be using on average half of the available resources [7]. Transmitted signals are subjected to distance-based path loss and generic composite fading (fast fading and shadowing) as defined in Chapter 2 Section 2.2. Since the basic deployment scenario of LTE is assuming universal frequency plan, the interference from other cells is bound to affect the SINR at the cell edge and needs to be considered in the link budget. Thus tailoring the link budget around a target SINR is equivalent to finding the maximum cell range that would satisfy this target with an outage probability less than or equal to a defined value. We first derive the downlink budget of an isolated cell considering the SNR at the cell edge, then we derive the link budget for a cell surrounded by N interfering cells considering the SINR at the cell edge to capture the resulting noise rise in LTE. The cell edge user receives the required signal from the serving cell but also interference from the N other cells in the network. At the cell edge of an isolated LTE cell the SNR (γ') can be expressed as follows:

$$\gamma' = \frac{S}{\sigma^2} = \frac{T \cdot A \cdot L_s}{\sigma^2} \tag{3.1}$$

Where T is the transmit power dedicated tot eh cell edge user, L_s is the path loss between the serving cell s and the cell edge user, and A_s is the fading/shadowing gain on the corresponding radio link. The link budget is designed to secure a target SINR (γ_τ) at the cell edge; thus by equating the measured SINR to the target SINR we can find the maximum allowed path loss that would satisfy the

condition. Accordingly we set $\gamma' = \gamma_\tau$ and solve for L_s or the MAPL L'_m as follows:

$$L'_m = \frac{\gamma'_\tau \cdot \sigma^2}{T \cdot A_s} \tag{3.2}$$

The fading and/or shadowing of the link between the serving cell and the given user at the cell edge is represented via the random variable A_s which behaves according to a PDF $f_A(a)$. Consequently, the maximum allowed path loss L'_m between the serving cell and its edge user follows a distribution solely dependent on $f_A(a)$, with all other parameters being constants.

In a realistic LTE deployment scenario, the serving cell would be surrounded by many other LTE cells sharing the same bandwidth thus causing interference to each other. In this case, the target edge performance is measured through the SINR as follows, where η_n is the loading on neighbouring cells and T is the transmit power per radio link, both entities assumed the same among all cells:

$$\gamma = \frac{S_s}{\sigma^2 + \sum\limits_{n \neq s} \eta_n \cdot S_n} = \frac{T \cdot A_s \cdot L_s}{\sigma^2 + \sum\limits_{n \neq s} \eta_n \cdot T \cdot A_n \cdot L_n} \tag{3.3}$$

In a similar manner as done for an isolated cell, the measured SINR is equated with the target SINR ($\gamma = \gamma_\tau$) then we solve for L_s which leads to the maximum allowed path loss L_m as follows:

$$\begin{aligned} L_m &= \gamma_\tau \frac{\sigma^2 + \sum\limits_{n \neq s} \eta_n \cdot T \cdot A_n \cdot L_n}{T \cdot A_s} \\ &= \frac{\gamma_\tau \cdot \sigma^2}{T \cdot A_s} \left(1 + 1/\sigma^2 \sum_{n \neq s} \eta_n \cdot T \cdot A_n \cdot L_n \right) \end{aligned} \tag{3.4}$$

Comparing (3.2) to (3.4), the effect of neighbouring cells interference results in an additional noise to the maximum allowed path loss, referred to as noise rise (or interference degradation) as defined below:

$$\begin{aligned} \mu &= \frac{1}{1 + 1/\sigma^2 \sum\limits_{n \neq s} \eta_n \cdot T \cdot A_n \cdot L_n} \\ &= \frac{\sigma^2}{\sigma^2 + \sum\limits_{n \neq s} \eta_n S_n} \cdot \frac{S_s}{S_s} \\ &= \frac{\gamma}{\gamma'} \end{aligned} \tag{3.5}$$

In an isolated cell scenario μ would be unity and $L_m = L'_m$ otherwise an additional loss incurred due to the other cells interference, dependant on the cell loading,

thus limiting the maximum path loss further where $L_m = L'_m \cdot \mu$. Consequently, the maximum allowed path loss is a function of multiple random variables: the respective received signals from the serving cell and all interfering cells are all random variables that behave individually according to a PDF $f_A(a)$. However the joint impact of these signals follows a different distribution that is scenario dependent and needs to be identified.

3.2 LTE link budget analysis

For the given model, the link budget analysis will be used to determine the maximum allowed distance between neighbouring sites in such a way that capacity and quality constraints are still met. Although the link budget is essentially a coverage dimensioning tool, it is tailored though in view of capacity and quality of service constraints. Capacity is represented by the noise rise μ which is a function of loading η_n in neighbouring cells. Higher loading results in higher transmission on the downlink and consequently higher interference perceived by the users. Quality of service is captured by the setting of the target SINR γ_τ, conventionally defined through link level simulations which map the desired link bit error rate (BER) to a required SINR for a defined data rate under given channel models. Although the main factors shaping the LTE link budget are mostly comparable to GSM and UMTS link budgets, the complexity however in LTE arises in the computation of the noise rise as a function of cell loading and channel variations due to fading and shadowing. The impact of channel fading and cell loading on the interference degradation can be easily captured through monte carlo simulations for instance, but that would compromise the essence of the link budget analysis being purely analytical and fast in generating dimensioning results.

3.2.1 Signal to interference and noise ratio (SINR)

The SINR is the first link budget parameter that needs to be modeled and analysed. On the downlink, the SINR for the cell edge user served by cell s and interfered by $N-1$ cells denoted by n is defined as follows:

$$\gamma = \frac{S_s}{\sigma^2 + \sum\limits_{n \neq s} \eta_n \cdot S_n} = \frac{L_s \cdot T \cdot A_s}{\sigma^2 + \sum\limits_{n \neq s} \eta_n \cdot L_n \cdot T \cdot A_n} \tag{3.6}$$

The SINR is then a random variable γ affected by the channel fading characteristics of the desired signal as well as that of the neighbouring cells.

3.2.2 Noise rise

In the link budget, the capacity aspect is represented by the noise rise. The noise rise in a cellular network is the deterioration of the SNR due to co-channel interference from neighbouring cells as derived in Section 3.1. A cell edge user in cell s surrounded by $N-1$ interfering cells with equal cell load η_n suffers from a noise rise μ which is a function of η_n and the geometry of the network as demonstrated in Section 3.1:

$$\mu = \frac{\sigma^2}{\sum\limits_{n \neq s} \eta_n \cdot L_n \cdot T \cdot A_n + \sigma^2} \tag{3.7}$$

The noise rise measured by a cell edge user is thus a random variable affected by the channel fading characteristics of the serving cell and that of the neighbouring cells considering the loading factor.

3.2.3 Maximum allowed path loss (MAPL)

The first outcome of the link budget is the maximum allowed path loss (MAPL) shown below in dB. It indicates the maximum loss limit between transmitter and receiver (at the cell boundary) beyond which the outage probability will increase above the target. MAPL is thus a random variable L_m as defined below:

$$L_m = T + G_T - l - (\sigma^2 + 10 \cdot \log(A_s) + \nu + \mu + \gamma_\tau + M_d) \tag{3.8}$$

Where:

- T is the transmit power at the eNodeB in dBm.
- G_T is the antenna gain at the eNodeB in dBi.
- l is the cable and connector loss at the eNodeB in dB.
- σ^2 is the thermal noise power in the channel in dBm.
- $10 \cdot \log(A_s)$ is the fading factor affecting the wanted signal in dB.
- ν is the noise figure at the receiver (eUE) in dB. The receiver noise figure is a none ideal realisation of any receiver whereby the receiver amplifier tends to amplify low signals (e.g., noise) more than high signals (e.g. required signal).
- μ is the noise rise at the cell edge in dB.
- γ_τ is a design value for target SINR in dB.
- M_d is a design margin that could include, e.g., indoor penetration loss in dB.

3.2.4 Maximum allowed cell range

The ultimate outcome of the link budget analysis is the maximum allowed cell range, directly derived from the MAPL using the equation of the propagation model introduced in Chapter 2 and repeated below for reference with δ_0 set to one.

$$L = 10^{K/10} R^{-\alpha} \tag{3.9}$$

By replacing L by the MAPL variable L_m and solving for R as shown below:

$$R = 10^{\left(\frac{L_m + K}{10 \cdot \alpha}\right)} \tag{3.10}$$

3.3 Statistical link budget analysis (SLBA)

There are two types of fading that govern the signals' strength received at the cell edge coming from any of the cells in the network; these are the large scale fading or "shadowing" and the small scale fading or "fading". In order to design the statistical link budget for LTE, the first building block is finding how the uncorrelated channel variations from the serving sector and all interfering cells combine at the cell edge under different cell loading scenarios, thus finding a statistical model for the SINR and the noise rise. The derivation is done for two channel models: Rayleigh fading and composite fading represented with a gamma distribution (Section 3.3.2). The distribution of the maximum allowed path loss is derived as function of SINR or noise rise. A suitable propagation model is then selected and the distribution of the resulting cell range is derived from that of the MAPL in Section 3.3.4. In the statistical link budget analysis, the aim is to find the resulting distribution of the cell range as a function of fading on the wanted and interfering signals.

3.3.1 SINR: Statistical distribution

SINR is the key design target of the dimensioning exercise and is the most complex to capture since it is a function of the statistical fading on the serving cell channel and all interfering cells' channels. Nonetheless, a closed form for the SINR distribution assuming Rayleigh fading on all channels concerned is possible as shown in this section. We first assume Rayleigh fading with unity fading power such that the probability distribution function of the variable A_i is $f_{A_i}(a) = e^{-a}$ for all channels. Accordingly, the total power received from interfering cells I is the sum of $N-1$ independent random variables thus the distribution of I is the result of the convolution of $N-1$ distributions.

$$I = \sum_{n \neq s} I_n = \sum_{n \neq s} \eta_n \cdot L_n \cdot T \cdot A_n \tag{3.11}$$

Consequently the pdf representing the variations of the received signal from one source of interference S_n is as follows:

$$f_{S_n}(a) = \frac{1}{I_n} \cdot e^{-\frac{a}{I_n}} \tag{3.12}$$

To simplify the mathematical load of such an operation, we use the moment generating function (MGF) approach to transport the computation to the frequency domain thus transforming convolutions to multiplications. The $\mathrm{MGF}_S(x)$ of S_n is thus $\frac{1}{1-I_n x}$ and the $\mathrm{MGF}_I(x)$ of I is the product of $N-1$ moment generating functions as shown below:

$$\mathrm{MGF}_I(x) = \prod_{n \neq s}^{L} \frac{1}{1 - I_n x} \tag{3.13}$$

Using partial fraction expansion, the $\mathrm{MGF}_I(x)$ can be expressed as follows:

$$\mathrm{MGF}_I(x) = \sum_{n \neq s}^{N} \frac{c_n}{1 - I_n x} \tag{3.14}$$

$$c_n = \prod_{k \neq n}^{N} \frac{1}{1 - \frac{I_k}{I_n}} \tag{3.15}$$

Expressing the product as a sum weighted by constants c_n, the distribution of I can be derived by inverting $\mathrm{MGF}_I(x)$ as follows:

$$f_I(i) = \sum_{n=1}^{N} \frac{c_n}{I_n} \cdot e^{-\frac{i}{I_n}}; i \geq 0 \tag{3.16}$$

Let y and z be as follows:

$$Y = \sigma^2 + I \tag{3.17}$$

$$f_Y(y) = \sum_{n=1}^{N} \frac{c_n}{I_n} \cdot e^{-\frac{y}{I_n}} \cdot e^{\frac{\sigma^2}{I_n}}; y \geq \sigma^2 \tag{3.18}$$

$$Z = \frac{A_s}{y} \tag{3.19}$$

$$f_Z(z) = \int_{\sigma^2}^{\infty} y \cdot f_{A_s}(yz) \cdot f_y(y) dy \tag{3.20}$$

Then the SINR can be expressed as a function of z such that $\gamma = L_s \cdot T \cdot z$ and the distribution of SINR is as follows:

$$\begin{aligned} f_\gamma(\gamma) &= \frac{1}{TL_s} \cdot f_z(\frac{\gamma}{TL_s}) \\ &= e^{b_1 \gamma} \sum_{n=1}^{L} \frac{c_n}{I_n} \left(\frac{b_1}{b_2 \gamma + 1/I_n} + \frac{b_2}{b_2 \gamma + 1/{I_n}^2} \right) \end{aligned} \tag{3.21}$$

$$\tag{3.22}$$

where $b_1 = \frac{\sigma^2}{L_s}$ and $b_2 = \frac{1}{L_s}$. It should be noted that at this stage a closed form expression for the SINR distribution assuming composite fading is still not found.

3.3.2 Noise rise: Statistical distribution

The first step in the derivation of the statistical noise rise distribution is finding the distribution of total interference from all neighbouring cells $(N-1)$. If d_n is the distance between neighbour cell n and the cell edge user and A_n is the random variable representing the channel fading between them, then let I_n be the interference from neighbouring cell n and let I be the total interference from all neighbouring cells as in (3.11). Considering Rayleigh fading channel model first, A_n is thus assumed to follow an exponential distribution. Accordingly, I_n also follows an exponential distribution of mean $\lambda_n = \eta_n \cdot L_n \cdot T \cdot E[A_n]$ where $E[A_n]$ is the expected value of the random variable A_n. Consequently, I is the sum of $N-1$ independent exponential random variables and its moment generating function can be derived as follows:

$$\mathrm{MGF}_I(x) = \prod_{n \neq s}^{N} \mathrm{MGF}_{I_n}(x) = \prod_{n \neq s}^{N} \frac{1}{1 - x\lambda_n} \tag{3.23}$$

Assuming that all λ_n are distinct, and taking the inverse of $\mathrm{MGF}_I(x)$ after partial fraction expansion leads to:

$$f_I(i) = \sum_{n \neq s}^{N} \frac{c_n}{\lambda_n} e^{-\frac{i}{\lambda_n}} \tag{3.24}$$

where c_n are the resulting coefficients from partial fraction expansion. Replacing $f_\mu(\mu)$ in (3.7) yields the distribution of the noise rise under Rayleigh fading as follows:

$$\begin{aligned} f_\mu(\mu) &= \sigma^2 \cdot f_I(\sigma^2(\mu - 1)) && (3.25) \\ &= \sigma^2 \cdot \sum_{n \neq s}^{N} \frac{c_n}{\lambda_n} e^{-\frac{\sigma^2(\mu-1)}{\lambda_n}} && (3.26) \end{aligned}$$

To find the distribution $f_\mu(\mu)$ under composite fading, we approximate A_n with a gamma distribution with shaping parameter m_n and inverse scaling parameter k_n [20]. Then, I_n also follows a gamma distribution with shaping parameter m_n and inverse scaling parameter ζ_n as defined below, resulting in $f_{I_n}(i)$ where Γ represents the gamma distribution and g represents the gamma function.

$$\begin{aligned} \zeta_n &= 10^{K/10} \cdot {\delta_0}^{\alpha} \cdot T \cdot d_n^{-\alpha} \cdot k_n && (3.27) \\ f_{I_n}(i) &= \Gamma(m_n, \frac{1}{\zeta_n}) = \frac{\zeta_n^{m_n}}{g(m_n)} x^{m_n - 1} e^{-\zeta_n i} && (3.28) \end{aligned}$$

We assume that all ζ_n are positive distinct real numbers and impose the constraint that the m_n's are positive integers, not necessarily distinct. Each I_n is therefore the sum of m_n independent exponential random variables with mean $\frac{1}{\zeta_n}$. Applying the partial fraction expansion to the moment generating functions of the variables I_n and I, we obtain first the coefficients c_{nj} for all values of j between 1 and m_n that are then used in the statistical distribution of μ after some manipulations, as shown below:

$$f_\mu(\mu) = \sigma^2 \sum_{n=1}^{N} \sum_{j=1}^{m_n} \frac{(-1)^j c_{nj}}{(j-1)!} (\sigma^2)^{j-1} (\mu-1)^{j-1} e^{-\lambda_n \sigma^2 (\mu-1)} \tag{3.29}$$

3.3.3 MAPL: Statistical distribution

The MAPL at the cell edge indicates the loss limit between transmitter and receiver beyond which the outage probability will increase above the target. As demonstrated earlier in Section 3.2.3, the MAPL is a function of two variables: A_s, the fading on the wanted signal and μ, the noise rise. The SINR encapsulates both of these variables, hence expressing the MAPL as a function of SINR would result in dealing with a single variable which is more accurate in outage probability estimation.

$$\begin{aligned}
L_m &= \frac{\gamma_\tau \cdot \sigma^2}{T \cdot A_s \cdot \mu} \\
L_m &= \gamma_\tau \left(\frac{\sigma^2 + \sum\limits_{n \neq s} \eta_n \cdot T \cdot A_n \cdot L_n}{T \cdot A_s} \right) \\
L_m &= \gamma_\tau \cdot L_s \left(\frac{\sigma^2 + \sum\limits_{n \neq s} \eta_n \cdot T \cdot A_n \cdot L_n}{T \cdot A_s \cdot L_s} \right) \\
L_m &= \frac{\gamma_\tau \cdot L_s}{\gamma}
\end{aligned} \tag{3.30}$$

Thus, if a closed form pdf of γ is possible, the distribution of L_m can be derived as a function of γ referred to hereafter as *SLBA1* (3.31). Otherwise, the distribution of L_m can be derived as a function of μ only while accounting for the fading variable on the wanted signal through a margin. This method will be referred to as *SLBA2*(3.32).

$$f_{L_m}(l_m) = \frac{\gamma_\tau \cdot L_s}{l_m^2} f_\gamma \left(\frac{\gamma_\tau \cdot L_s}{l_m} \right) \tag{3.31}$$

$$f_{L_m}(l_m) = \frac{\Omega}{l_m^2} f_\mu \left(\frac{\Omega}{l_m} \right) \tag{3.32}$$

3.3.4 Cell range: Statistical distribution

As a final result, the distribution of the cell range, R, is directly derived from L_m as defined in (3.10) and can thus be expressed as follows:

$$f_R(r) = \xi \cdot \alpha \cdot r^{\alpha-1} \cdot f_{L_m}(\xi \cdot r^{\alpha}) \quad (3.33)$$

$$\xi = \frac{1}{10^{\frac{K}{10}}} \quad (3.34)$$

3.4 Results and analysis

In this section, we will demonstrate the usage of the derived distributions in LTE radio dimensioning, and draw insights and guidelines pertinent to LTE dimensioning under statistical interference modeling and varying traffic demand. The derived distributions are first compared to monte carlo simulations for validation. Three scenarios are considered: Rayleigh fading and composite fading with an aggregate shaping factor equal to one and two. Two tiers of three sectored sites are considered thus one serving cell and 56 interfering cells affect the received SINR at the cell edge. Other key parameters are listed in Table 3.1. It should be noted that the eNodeB power is amplified by the transmit antenna and reduced due to the cable loss; thus the effective isotropic radiated power (EiRP) is calculated instead of transmission power. Moreover, the EiRP per subcarrier is then computed assuming equal distribution of power among the sub-carriers.

3.4.1 Validation of derived distributions

The initial step is to validate the derived distribution against monte carlo simulations assuming both Rayleigh and composite fading. Results are shown in Figure 3.2, where a cell load of 50% is assumed in the nine sub-figures representing the noise rise, MAPL, and cell range for Rayleigh, composite fading with shaping factor (SF) set to 1, and composite fading with shaping factor set to 2, respectively. As can be seen, the three derived dimensioning-related distributions in Section 3.3 match very well monte carlo simulation (10000 iterations) results for both channel fading models; this validates the accuracy of the derived expressions.

3.4.2 Comparison of SLBA1 and SLBA2

As presented in Section 3.3.3, the SLBA2 approach is proposed as an alternative to the SLBA1 approach in case a manageable closed form of SINR distribution is difficult to reach. In this section we aim at evaluating the validity of this proposal by comparing the results obtained from both approaches. As shown in Figure 3.3 the actual standard deviation of the cell range distribution resulting from SLBA1 is much larger than that obtained from SLBA2. This is a normal outcome since,

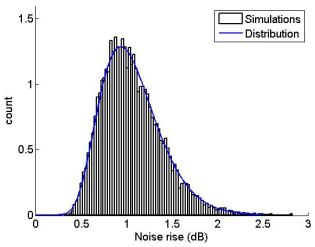

(a) Rayleigh fading: Noise rise distribution.

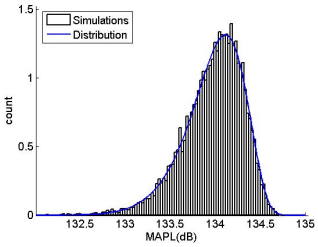

(b) Rayleigh fading: MAPL distribution.

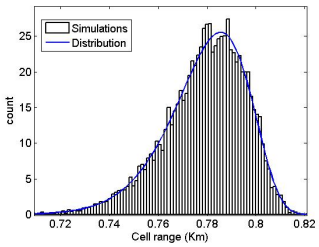

(c) Rayleigh fading: Cell range distribution.

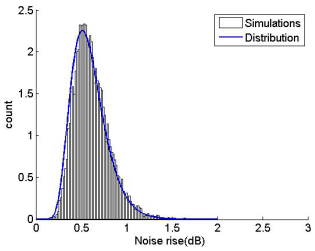

(e) Composite fading (SF=1): Noise rise distribution.

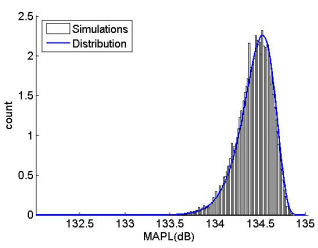

(f) Composite fading (SF=1): MAPL distribution.

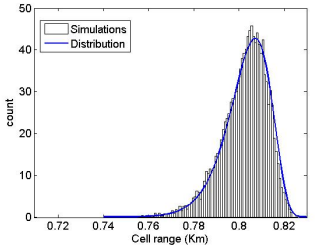

(g) Composite fading (SF=1): Cell range distribution.

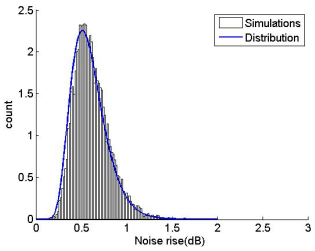

(e) Composite fading (SF=2): Noise rise distribution.

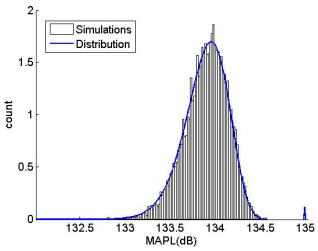

(f) Composite fading (SF=2): MAPL distribution.

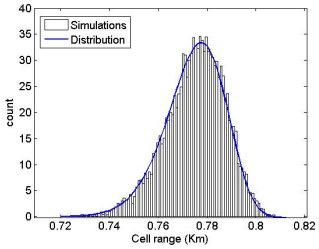

(g) Composite fading (SF=2): Cell range distribution.

Figure 3.2: Comparison between derived distributions and simulation results.

Table 3.1: Network parameters and assumptions.

Parameters	**Unit**	**Expression**	**Value**
Total Transmit Power	dBm	P'	46
TX Antenna Gain	dBi	G_T	18
Cable/Connector/Combiner Losses	dB	l	2.5
EiRP	dBm	$d = P' + G_T - l$	61.5
Total number of sub-carriers	10MHz	H	600
Tx EiRP per sub-carrier	dBm	$P = 10 \cdot \log(\frac{10^{\frac{d}{10}}}{H})$	33.7
Thermal Noise Density	dBm/Hz	f	-173.8
Bandwidth per sub-carrier	Hz	W	15000
Total Thermal noise in channel	dBm	$\sigma^2 = f + 10 \cdot \log(W)$	-132.0
RX Antenna Gain	dBi	G_1	0
RX Noise Figure	dB	L_1	7
Required SINR at cell Edge	dB	γ_τ	-2.1
Penetration Loss	dB	L_2	18

in SLBA2, a major variable is replaced by a fixed margin hence the resulting cell range varies less than the one obtained with SLBA1. Moreover, SLBA2 distributions with different fading margins are displayed to find the appropriate margin to be used in the approximation method. It is evident that an exaggerated margin (e.g., 5 dB and 8 dB) would result in pessimistic cell range and thus over-dimensioning of the network. On the other hand, a lenient margin (e.g., 0 dB) would result in optimistic cell range and thus under-dimensioning of the network. In the given example, the appropriate safe M_f that should be used with SLBA2 is 3 dB as can be seen from Figure 3.3 and yields a cell range equal to 1 km, the same as the result found using SLBA1 assuming a target ECP equal to 65%. Furthermore, if SLBA2 were to be used instead of SLBA1, the safe fading margin M_f would need to be recalculated for different cell edge coverage probability target, different cell load and different network geometry. However, one has to take care in radio network planning when more than one power margin is used. For instance, the overall margin M_t in the traditional link budget will be equal to $M_f + M_i$ and the overall outage probability for the worst case user will be $P_{out} = 1 - (1 - P_{out1})(1 - P_{out2})$, where P_{out1} and P_{out2} are the outages due to shadowing and interference degradation respectively. If each of M_f and M_i is selected for an outage probability of 5% then the real total outage probability will be around 10% [21]. Another essential remark to add at this stage is that the RND approach established in this research remains valid for both SLBA1 and SLBA2. When a closed form SINR distribution is found it can be plugged into the procedure which would automatically adapt to it.

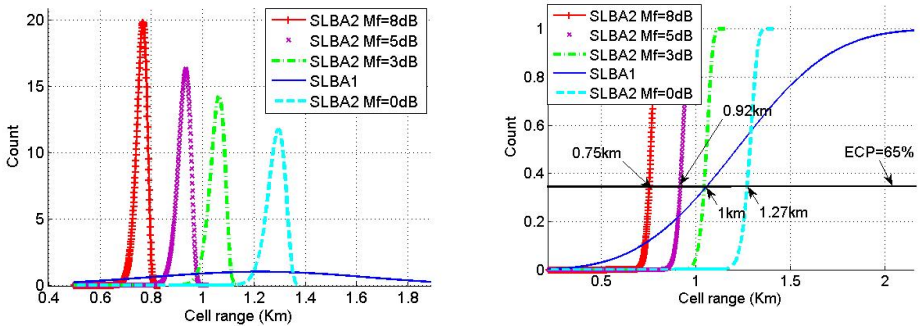

(a) PDF of cell range using SLBA1 and SLBA2.

(b) CDF of cell range using SLBA1 and SLBA2.

Figure 3.3: Comparison between SLBA1 and SLBA2 results.

3.4.3 Tradeoff analysis and insights

In order to explore the tradeoff characteristics inherent to LTE technology, we use the cell range distribution from the SLBA approach. The effect of cell loading is demonstrated in Figure 3.4 which presents the probability distribution function (PDF) cumulative distribution function (CDF) of the cell range. The inter-site distance is fixed to 1.3 km which corresponds to a cell range of 0.75 km. The variable loading on the neighbouring cells is seen to engender two phenomena: greater *elasticity* due to amplified channel variations and *breathing* due to increased load. Higher cell load results in wider cell range variations around the mean; this indicates that at high load, the aggregate effect of channel variations from the serving cell and the neighbouring cells amplifies the SINR fluctuations at the cell edge; this effect is referred to as cell elasticity. On the other hand, the increased cell load moves the mean of the statistical cell radius towards smaller ranges; a phenomenon referred to as cell breathing.

Referring to Figure 3.4 (a), the vertical line at 0.75 km cell range is the actual footprint of the cell hence the cell edge user is located at 0.75 km from the serving base station. For a 10% cell load the CDF shows 0% probability for cell ranges lower than 0.75 km, thus, the cell edge user achieves the target SINR 100% of the time. The probability decreases with increasing cell load resulting in 98% coverage probability at 30% cell load, 71.3% coverage probability at 50% cell load, 34.6% coverage probability at 70% cell load, and 13% coverage probability at 90% cell load (Figure 3.4 (b)). If, for instance, the worst case scenario (i.e., full load) was considered the resulting network will be over-dimensioned thus incurring unjustified increase in capital expenditure and operational cost (refer to Figure 3.6 right-side).

Another critical aspect that can be drawn is the drastic impact of inter-site distance on the cell edge user performance as shown in Figure 3.5 which presents

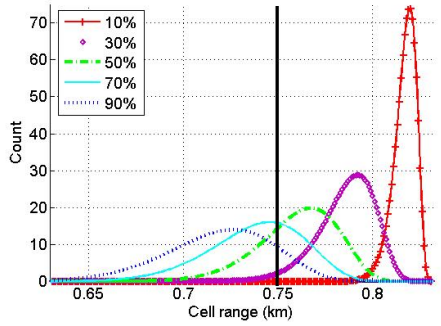

(a) PDF of effective cell range at different loadings.

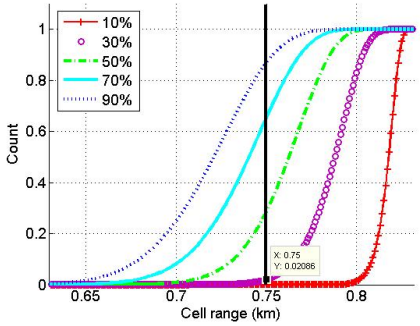

(b) CDF of effective cell range at different loadings.

Figure 3.4: Effect of cell loading on cell range distribution. The inter-site distance in all cases is 1.3 km.

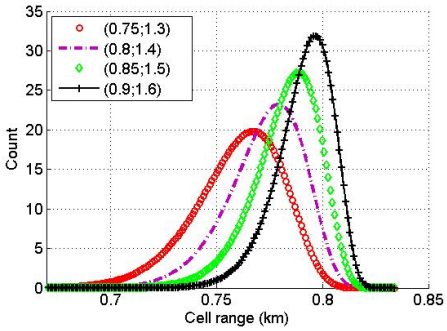

(a) PDF of effective cell range at difference inter-site distances.

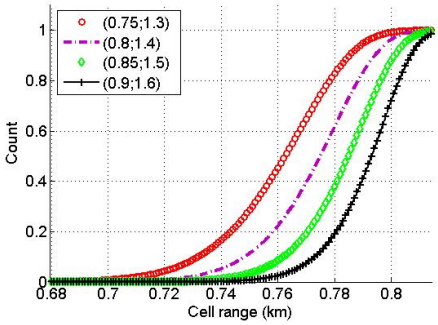

(b) CDF of effective cell range at difference inter-site distances.

Figure 3.5: Effect of inter-site distance on cell range distribution. The values in brackets in the legend correspond to (presumed cell range; inter-site distance). Cell load fixed at 50%.

the cell range PDF and CDF under different settings. The statistical cell range actually varies around the fixed cell range dictated by the inter-site distance. Figure 3.5 (a) shows that changing the inter-site distance from 1.3 km to 1.6 km reduces the chances of an edge user achieving the required data rate or γ_τ while the cell load is constant at 50%. Referring to Figure 3.5 (b) and looking at the CDF curve corresponding to 1.3 km inter-site distance or 0.75 km cell range, we find that the effective cell range varies, and its probability of being equal to or higher than 0.75 km is about 71.3%. This probability reduces though to less than 5% when the inter-site distance increases to 1.4 km as indicated by the probability of the effective cell range being equal to or higher than 0.8 km (corresponding cell range). It is thus of major importance to tune the inter-site distance to the statistical cell range and consequently find the optimal distance between sites that would reduce the performance degradation at cell borders.

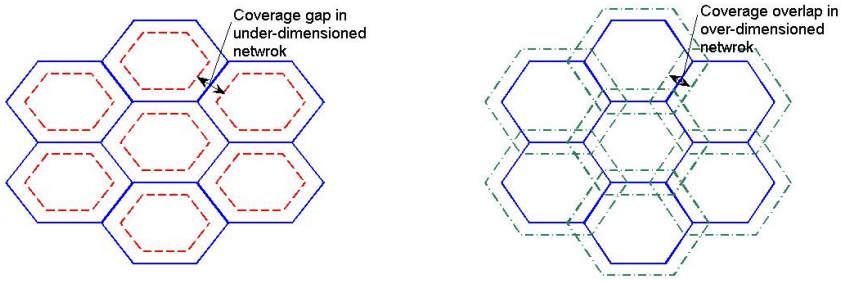

(a) Under-dimensioned network.

(b) Over-dimensioned network.

Figure 3.6: The figure on the left side shows an under-dimensioned network; the figure on the right shows an over-dimensioned network.

Moreover, the setting of the inter-site distance is very sensitive whereby a mere 100 meters increase would degrade the cell edge performance below acceptable levels.

Chapter 4

Statistical Analysis of LTE Dimensioning (SALTED) Tool

In Chapter 3 we have presented a statistical approach for interference modeling in an LTE network which lead to the derivation of statistical distributions of key dimensioning entities namely SINR, noise rise, maximum allowed path loss and cell range. The causal relations between capacity, coverage and quality that have been drawn, highlight the need for accurate considerations of capacity demand in the link budget analysis and uncover severe performance degradation that may result from pragmatic assumptions. The results presented thus promote the development of a complete statistical link budget analysis approach that adapts to the varying system interference as well as traffic demand to yield an optimised design in inter-site distance selection and network parameter selection. Accordingly, an iterative algorithm that is based on the SLBA approach is developed and tested with the aim of balancing coverage, quality and capacity demands in an LTE network.

The resulting iterative process is implemented in a user friendly tool with main GUI designed in Visual Basic Application (VBA) and close interaction with Matlab. The tool is called **S**tatistical **A**nalysis of **LTE D**imensioning (**SALTED**). The purpose of developing SALTED is to automate the tuning process and facilitate the implementation of diverse what/if scenarios to explore the intrinsic characteristics of LTE dimensioning.

4.1 Iterative process for LTE dimensioning

The SLBA approach drawn in Chapter 3 forms the basic module in the iterative process proposed. When applicable (i.e., when a closed form SINR distribution function is available), either SLBA1 or SLBA2 can be selected; otherwise only SLBA2 is possible. The iterative algorithm is shown in Figure 4.1. The process

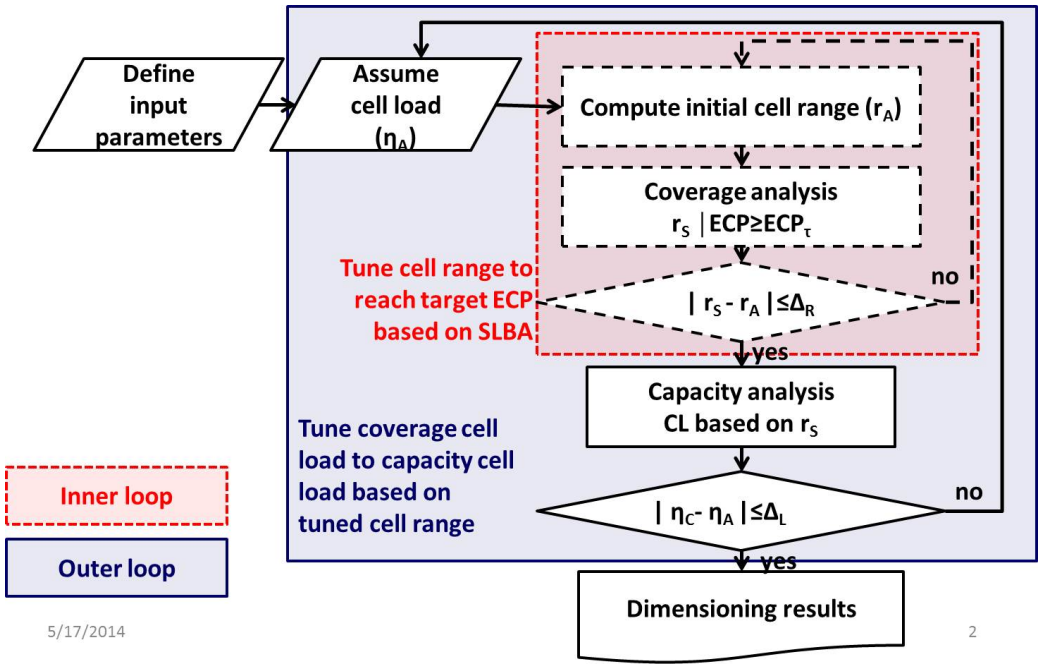

Figure 4.1: SLBA-based process for LTE dimensioning.

starts by setting input parameters that are deterministic and user defined. A cell load η_A is then assumed and the traditional link budget is used to find an approximate corresponding cell range r_A. Then the inner loop is initiated which attempts to find the best inter site distance that would provide the required edge coverage probability (ECP), and calculated the safe cell range r_S which corresponds to this inter-site distance. When the difference between r_A and r_S is below a user defined target Δ_R, the inner loop reaches convergence, upon which the capacity analysis is initiated. The capacity analysis gives the cell load based on the cell range r_S which is identified as η_C. If the difference between the assumed cell load η_A and the capacity cell load η_C is within the user defined error margin Δ_L, then the outer loop has converged, otherwise it will iterate until the convergence target is reached by modifying the assumed the cell load each time. It should be noted that for each iteration of outer loop, the inner loop iterates until convergence. Moreover, there a user defined upper limit on the number of iterations per inner loop and per outer loop which would halt the process even if there is no convergence.

The algorithm proposed is implemented in Matlab and takes a set of input parameters as listed in Table 4.1. In addition to that, some functions are hardcoded such as the mapping between number of sectors and area coefficient (Table 4.2). The area coefficient is used to compute the effective site density (Σ) based on the number of sectors as: $\Sigma = \frac{1}{C_A \cdot r^2}$. Table 4.3 shows the hardcoded mapping between allocated spectrum and number of sub-carriers based on LTE specifications.

Table 4.1: Input parameters to SLBA-based iterative process.

Parameters	**Unit**	**Value**
Total transmit power	dBm	46
TX antenna gain	dBi	18
Cable/Connector/Combiner Losses	dB	2.5
Spectrum	MHz	10
Thermal noise nensity	dBm/Hz	-173.8
Bandwidth per sub-carrier	Hz	15000
RX noise figure	dB	7
Required SINR at cell edge	dB	-2.1
Penetration loss	dB	18
Fading margin	dB	3
Number of sectors		3
Acceptable error on cell load	%	1
Acceptable error on cell range	m	10
Maximum number of outer loop iterations		50
Maximum number of inner loop iterations		50

Table 4.2: Mapping between number of sectors and area coefficient.

Number of Sectors	Area coefficient
1	2.6
3	1.95
6	2.6

4.2 Results from SLBA-based iterative process

For a given set of input parameters, the main dimensioning output is summarised in Table 4.4. In the example shown,the SALTED algorithm has converged for both inner and outer loops, and the tuned cell range and corresponding cell load are indicated. In addition, the SALTED algorithm provides the actual edge coverage probability that may differ from the target but should not exceed the target. In the example shown, the design is coverage limited which means that the maximum cell ranged is determined by propagation constraints. If the design were capacity limited, attenuation factor would be added gradually to the link budget to reduce the transmit power and reach convergence with capacity limitations. Beside, optimisation indicators are reported for total number of iterations and time required to reach convergence. With the set of output results listed, a sensitivity analysis is conducted to further understand the interdependencies between pertinent LTE dimensioning parameters. Looking at Figure 4.2 (a), it can be seen that increasing the target edge coverage probability (ECP) reduces the cell range which is an expected consequence since more stringent quality requirements

Table 4.3: Mapping between allocated spectrum and number of sub-carriers.

Allocated spectrum (MHz)	Number of resource blocks	number of sub-carriers
1.4	6	72
3	15	180
5	25	300
10	50	600
15	75	900
20	100	1200

Table 4.4: Example dimensioning output resulting from SLBA-based iterative process.

Output parameter	Example value
Cell range (km)	0.83
Actual cell load (%)	35.83817
Actual edge coverage probability (%)	69.77105
Attenuation (for capacity limited design) (dB)	0
Tuning time (sec)	71.12534
Number of total iterations	17

at the cell edge necessitate that the cell edge be closer to the site. Figure 4.2 (b), resulting cell load which increases as the cell range increases because more subscribers are captures and the capacity of the cell approaches saturation..

Figure 4.3 (a) shows the impact of eNodeB maximum PA power on cell range which increases with additional power until the design becomes capacity limited. Figure 4.3 (b) shows the effect on cell range which reaches 100% whne the design becomes limited by maximum cell capacity. In Figure 4.3 (c) the resulting added attenuation is shown which is introduced to the link budget to reduce the cell range to tune coverage and capacity constraints.

4.3 SALTED implementation

The process presented in Section 4.1 is implemented in a user friendly tool, SALTED, in VBA and Matlab. The functional blocks of SALTED are shown in Figure 4.4. The entry point is an excel file, *SLBA.xlsm*, which is predefined with default dimensioning parameters and is used for data storage.
The core of SALTED is a Matlab function *SLBA-mat* that computes the statistical "tuned" cell range given a set of input parameters. The tuned cell range is calculated from the optimised inter-site distance that insures equilibrium between coverage and capacity considerations while respecting quality requirements. The

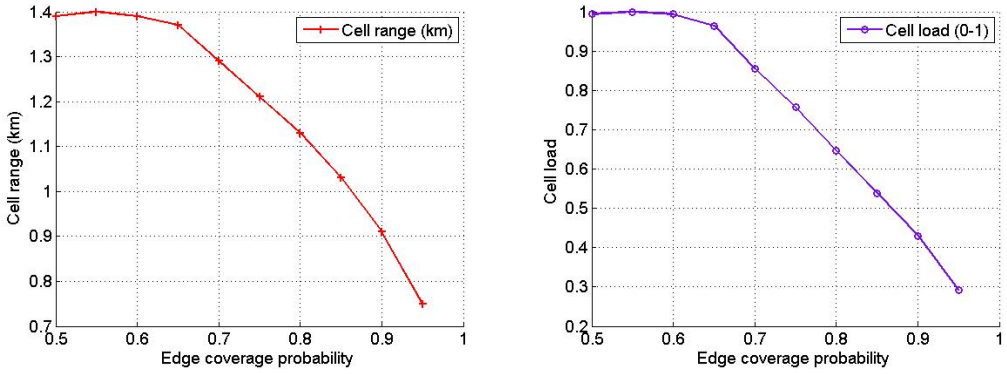

(a) Cell range. (b) Cell load.

Figure 4.2: Effect of target ECP on dimensioning results; cell range and consequently cell load decreased with more stringent ECP target.

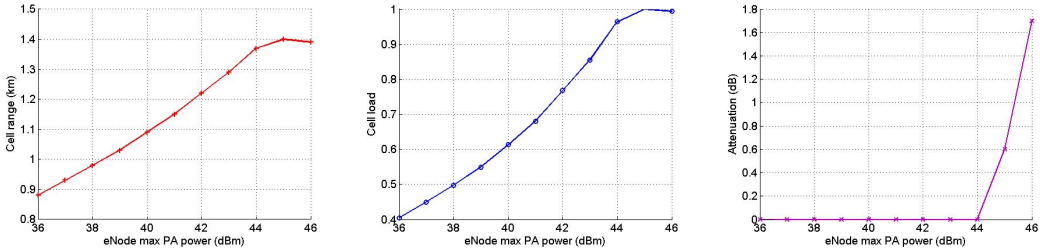

(a) Cell range. (b) Cell load. (c) Attenuation.

Figure 4.3: Effect of PA power on dimensioning results; cell range and consequently cell load increase with added power until the design becomes capacity limited. At this point added power is met with added attenuation to keep the balance of coverage and capacity constraints.

optimised inter-site distance is reached through an iterative process that has an inner loop and an outer loop. The outer loop aims at adjusting the assumed cell load from the capacity analysis to closely approach the cell load from the coverage analysis. The inner loop aims at adjusting the inter-site distance to the statistical cell range resulting from the coverage and quality analysis. Figure 4.1 depicts the interaction between the outer and inner loop.

The main GUI of SALTED is designed in VBA as shown in Figure 4.5 (a), and allows four options: SLBA, Sensitivity analysis, View results, and Quit. If SLBA is selected a interactive window opens as shown in Figure 4.5 (b) that suggests default values and allows the user to edit and save or perform SLBA dimensioning by choosing *Run*.

Running SLBA will call the Matlab function *SLBA-mat* to reach the "tuned" cell range, and subsequently another Matlab function, *SLBA-cov* will be called to generate coverage plots based on the dimensioning results from *SLBA-mat*.

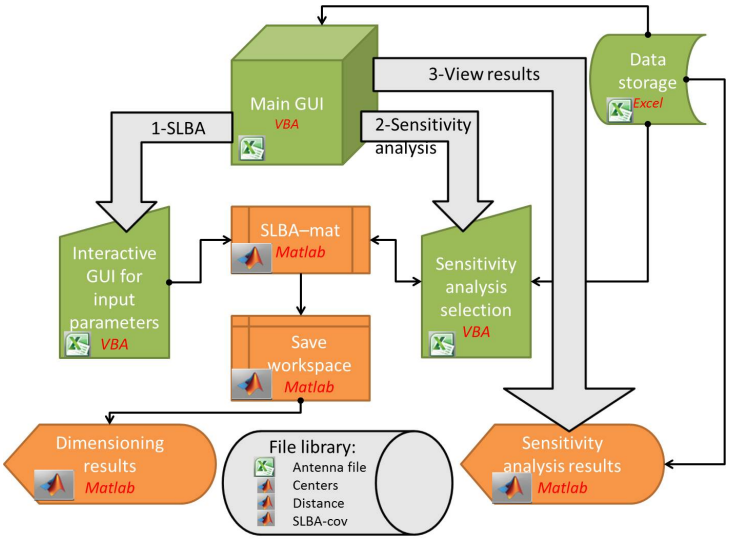

Figure 4.4: The storage and basic user interface of SALTED are implemented with Excel/VBA. The statistical derivations and iterative processes are implemented in Matlab. .

A Matlab GUI is used to display the dimensioning results from both *SLBA-mat* and *SLBA-cov* as shown in Figures 4.6, 4.7, and 4.8.

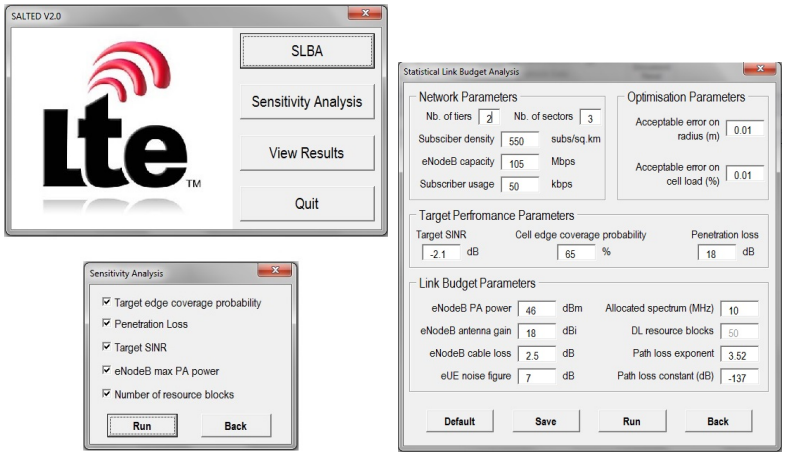

(a) SLBA main and sensitivity analysis windows.

(b) SLBA interactive parameter definition window.

Figure 4.5: The upper window is the main SALTED GUI which provides three options. The lower left window opens if sensitivity analysis is selected and provides the user with choice of parameters to vary and measure their effect on cell range. The right most window is the main input window which retrieves stored data and allows modifications. The input parameters are used for SLBA and sensitivity analysis options.

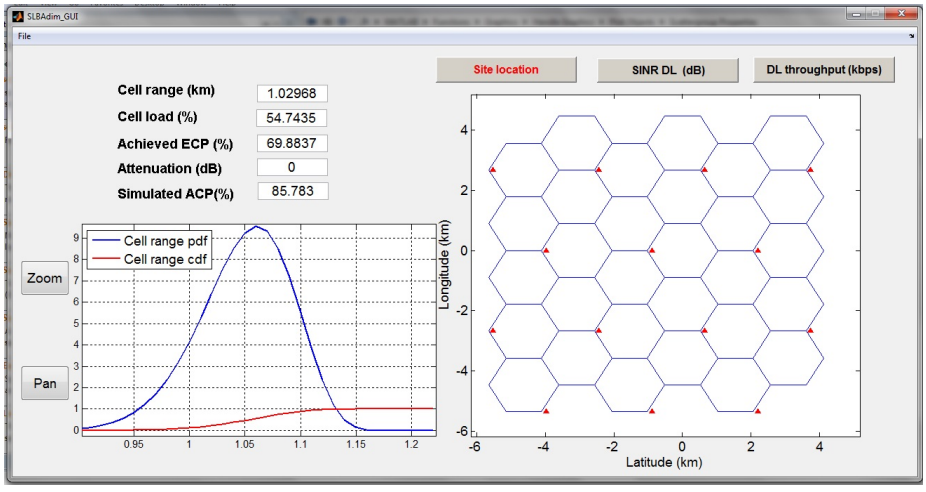

Figure 4.6: SLBA default output showing the statistical cell range in the left side figure and the sites positions in the right side figure. The main dimensioning results are reported in the left upper corner of the window. The output GUI allows the user to zoom and pan to improve plot visibility.

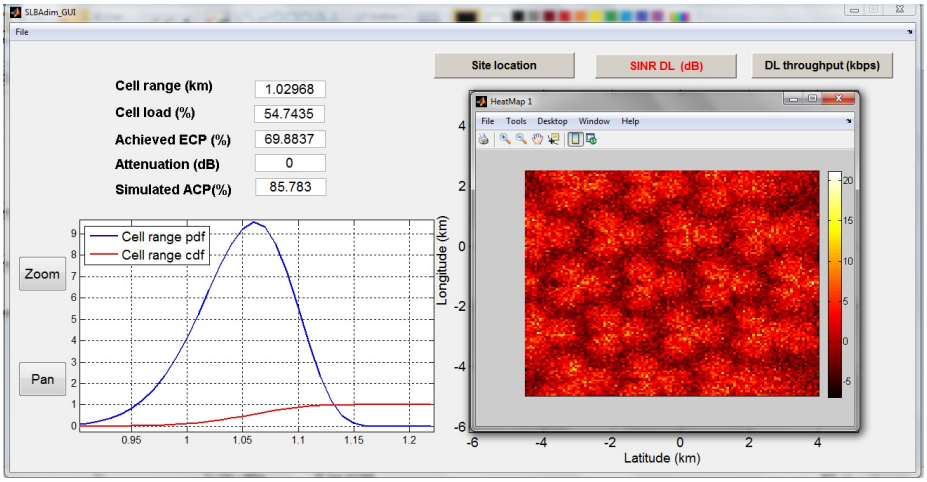

Figure 4.7: SLBA output GUI allows the user to display the coverage plot of DL SINR in dB using Matlab HeatMap function. This coverage plot is reached using the "tuned" inter-site distance and running monte carlo simulations. The simulated area coverage probability (ACP) is thus the ratio of points achieving the required SINR in the area considered.

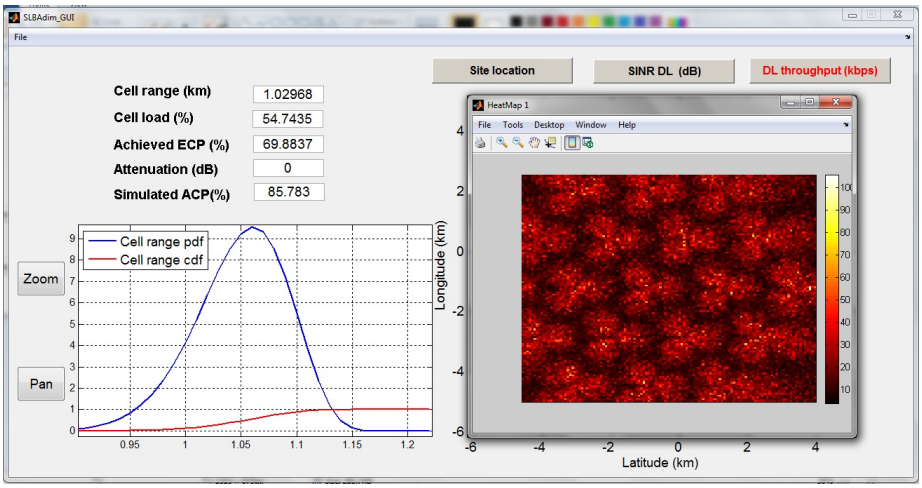

Figure 4.8: SLBA output GUI allows the user to display the coverage plot of DL throughput in kbps assuming single subcarrier per user, using Matlab HeatMap function. This result is based on the SINR coverage map in Figure 4.8 using Shannon theorem $C = B \cdot \log(1 + \gamma)$ where C is the DL throughput, B is the bandwidth of one subcarrier and γ is the linear SINR value.

Chapter 5

Case study

In this chapter we aim at benchmarking *SALTED* results against traditional LTE dimensioning approach with the use of a professional LTE planning tool, Mentum Planet [22]. A case study is thus proposed in which the same set of input parameters is used in the traditional approach, *SALTED*, and Mentum Planet and the dimensioning results are compared.

Table 5.1: Network parameters and assumptions.

Coverage Parameters	**Unit**	**Value**
Total transmit PA power	dBm	46
TX antenna gain	dBi	18
Cable/Connector/Combiner losses	dB	2.5
Total number of sub-carriers	10MHz	600
Thermal noise density	dBm/Hz	-173.8
Bandwidth per sub-carrier	Hz	15000
RX antenna gain	dBi	0
RX noise figure	dB	7
Penetration loss	dB	18
Quality Parameters	**Unit**	**Value**
Target area	km^2	66
Required SINR at cell edge	dB	-2.1
Edge coverage probability	%	65
Capacity Parameters	**Unit**	**Value**
Subscriber density	sub/km^2	550
Sector capacity	Mbps	35
Subscriber usage	kbps	50
Propagation Parameters	**Unit**	**Value**
Propagation exponent	dB/decade	35.2
Propagation constant	dB	-137

5.1 Traditional LTE dimensioning

As presented in Chapter 2, in the traditional approach a margin, M_f is typically derived assuming that the random variable A_s follows a log-normal distribution with an area specific shadowing standard deviation to guarantee the target coverage probability. The noise rise is often accounted for through an interference degradation margin M_μ typically 1-4 dB. Thus the link budget can be designed as in Table 5.2.

Table 5.2: Traditional LTE dimensioning results.

Link budget parameters	**Unit**	**Formula**	**Value**
Total Transmit Power	dBm	P'	46
TX Antenna Gain	dBi	G_T	18
Cable/Connector/Combiner Losses	dB	l	2.5
EiRP	dBm	$d = P' + G_T - l$	61.5
Total number of sub-carriers	10MHz	H	600
Tx EiRP per sub-carrier	dBm	$P = 10 \cdot \log(\frac{10^{\frac{d}{10}}}{H})$	33.7
Thermal Noise Density	dBm/Hz	f	-173.8
Bandwidth per sub-carrier	Hz	W	15000
Total Thermal noise in channel	dBm	$N_t = f + 10 \cdot \log(W)$	-132.0
RX Antenna Gain	dBi	G_1	0
RX Noise Figure	dB	L_1	7
Required SINR at cell Edge	dB	γ_τ	-2.1
Penetration Loss	dB	L_2	18
Total gains	dB	$M_G = G_1$	0
Total losses	dB	$M_L = L_1 + L_2$	25
Shadowing margin	dB	M_f	5
Interference degradation margin	dB	M_μ	2
Total design margin	dB	$M_t = M_G + M_L + \gamma_\tau + M_f + M_\mu$	29.9
Dimensioning results	**Unit**	**Formula**	**Value**
MAPL	dB	$L_m = P - (N_t + M_t)$	135.8
Cell range	km	$R = 10^{\frac{L_m - K}{10\alpha}}$	0.931
Site area coefficient		S_c	1.95
Site density	sites/km^2	$D_s = 1/(S_c \cdot R^2)$	0.592
Number of required sites	sites	$eN_b = \Lambda \cdot D_s$	39

5.2 SALTED dimensioning

The same design assumptions and targets are used in *SALTED* with additional simulation parameters as defined in Table 5.3. The simulation results are sum-

marized in Table 5.4 and the resulting coverage maps are shown in Figure 5.1.

Table 5.3: SALTED additional simulation parameters.

Simulation parameters	**Unit**	**Value**
Accepted error on cell range (Inner loop)	m	10
Accepted error on cell load (Outer loop)	%	1
Attenuation step	dB	0.1

Table 5.4: SALTED results.

Simulation results	**Unit**	**Value**
Number of iterations	Total	10
Simulation time	sec	41.7
Cell range	km	1.026
Cell load	%	54.75
Actual edge coverage probability	%	67
Required attenuation	dB	0
Dimensioning results	**Unit**	**Value**
Site area coefficient		1.95
Site density	sites/km^2	0.487
Number of required sites	sites	32

5.3 Mentum Planet dimensioning

Mentum Planet is a professional planning tool used by operators and telecom vendors alike in planning real cellular network deployments ranging from GSM to LTE including fixed wireless, WiMAX, FDD and TDD technologies. Mentum Planet 5.5.0.352-Educational Edition-LTE FDD is used in this exercise to benchmark results from both the traditional and the SALTED dimensioning approaches. The tool is used together with a 20m resolution digital terrain map of greater Beirut and the focus area is selected to be Ras Beirut as shown in Figure 5.2.

5.3.1 Mentum Planet settings

Mentum Planet, like any other planning tool, computes propagation loss based on a digital terrain map and takes into consideration terrain height to analyse diffraction losses and uses clutter classification to adjust propagation losses according to additional clutter absorbtion loss. For the purpose of our exercise, we selected an area in Beirut that is relatively flat as depicted in Figure 5.2 (a)

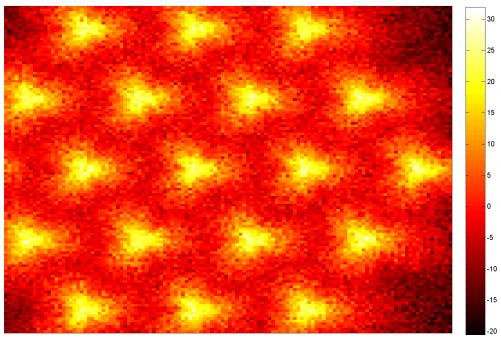

(a) SINR heat map (dB).

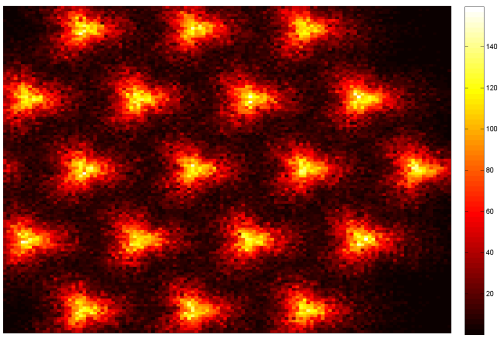

(b) DL throughput heat map (kbps).

Figure 5.1: Coverage maps assuming results obtained from SALTED as listed in Table 5.4. These coverage maps are generated with monte carlo simulations assuming the same parameters as those used for dimensioning SALTED and the resulting inter-site distance and attenuation factor if any.

to minimise the sources of difference when comparing simulation results to those obtained by both SALTED and the traditional approach.

The selected area is highlighted in blue in Figure 5.2 (b), and as seen in Figure 5.2 (c), the area covers a diverse range of varied clutter types ranging from core urban to suburban and forests. In a real life application, and extensive carrier wave measurement campaign is conducted to fine tune the clutter absorbtion losses that correspond to each clutter class which are later used in the propagation loss computation. Since this level of detail is overlooked in RND, all clutter classes will be assumed to have zero absorption loss in our simulations to enable fair comparison.

Moreover, clutter classification is often used in real network planning exercises to bias the subscriber distribution and respective cellular network usage accordingly. For instance, it is normal to assume higher subscriber density in dense urban areas compared to villages; also it may be assumed that subscribers in industrial areas have higher usage to cellular services considering they are professionals who's phone bill is covered by their employer. However, this option of uneven subscribers is omitted and uniform distribution is assumed throughout the focus area for fair comparison.

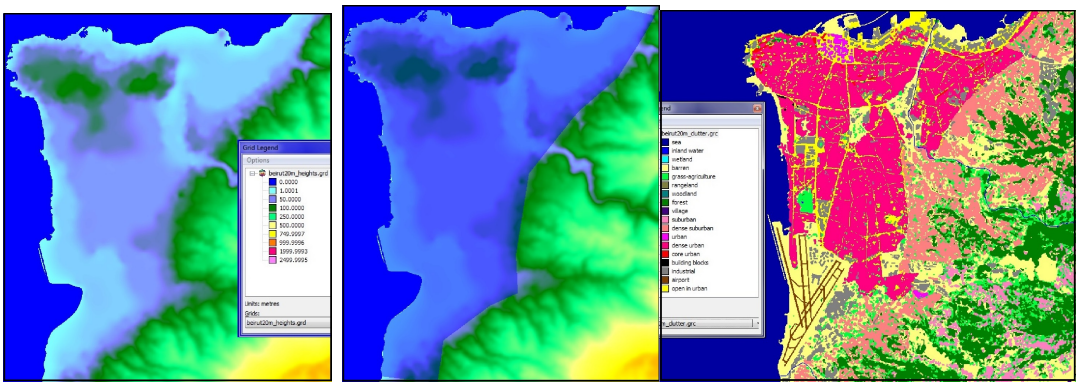

(a) Height map of Ras Beirut. (b) Focus area of Ras Beirut covering 66 km^2. (c) Clutter map of Ras Beirut.

Figure 5.2: Area of Ras Beirut considered int eh case study.

5.3.2 Planning methodology

The automatic site planning option of Mentum Planet is selected for this exercise since it is the closest to dimensioning. In this option, the cell range is user defined and the focus area (refer to Figure 5.2) is filled automatically by equally distant and identical sites. Due to the random shape of the focus area, it is expected that some regions in the boundaries would not be properly covered and possibly some sectors in boundary sites would be redundant. However, to enable fair comparison, no further optimisation is performed on the sites' locations to improve coverage in either scenarios.

Moreover, pertinent parameters such as spectrum allocation, propagation model coefficients, antenna gain pattern and power settings are adjusted in Mentum Planet to match the assumptions used in the case study (refer to Table 5.1). For some parameters however, the tool does not allow complete synchronisation most importantly in the channel fading settings. For other parameters, such as terrain height and mapping between SINR and data throughput, the default settings were kept. The only modification that is user defined in Table 5.5 is the minimum value of SINR that is changed from the default -1.1 to -2.1 dB. Accordingly, although there are a few uncontrolled sources of discrepancy in the network settings, the assumptions are nonetheless mostly synchronised between analytical dimensioning and Mentum Planet dimensioning.

5.3.3 Results from Mentum Planet

The cell range that resulted from the traditional link budget analysis, as derived in Table 5.2 is first fed to the automatic cell planning (ACP) tool in Mentum

Table 5.5: Modulation and coding scheme mapping to SINR table in Mentum Planet.

MCS	Useful bits per symbol	Required SINR (dB)
QPSK-1/3	0.67	-2.1
QPSK-1/2	1	1
QPSK-2/3	1.33	3
QPSK-4/5	1.6	4.5
16QAM-1/2	2	6.2
16QAM-2/3	2.67	7.5
16QAM-4/5	3.2	10.8
64QAM-2/3	4	14.2
64QAM-4/5	4.8	16.9

Planet; the outcome is 30 created sites as shown in Figure 5.3 (a). Then the cell range that resulted from SALTED (Table 5.4) is used together with the ACP tool, consequently, 22 sites are generated as shown in Figure 5.3 (b). It is interesting to note that the ACP tool in Mentum Planet resulted in 9 less sites compared to the number in Table 5.2 which is mostly due to the approximation taken in the area coefficient consideration in the the SLBA, but also as a side effect to the form of the focus area. In the SALTED scenario, as well, 10 less sites are created by ACP compared to Table 5.4.

LTE analysis of both scenarios is conducted in Mentum Planet and the results are compared. Since the dimensioning approach presented in this work is mainly for the downlink, only downlink results are inspected. Moreover, performance of the design is measured against the target SINR on the downlink, set to -2.1dB in the quality section in Table 5.1, and entered in the MCS table in Mentum Planet 5.5. SINR coverage maps are shown in Figures 5.3 (a) and 5.3 (b) for the traditional and SALTED scenarios respectively; they are summarised in a pie chart in Figure 5.4 for more clarification.

The monte carlo simulation generates several iterations of subscriber spreading until the results converge to a user defined target. The results are shown in Figure 5.5 (a) and Figure 5.5 (b) for the traditional and SALTED scenarios respectively; subscribers are depicted by a green diamond if they have coverage, blue if the they are out of coverage due to lack of downlink power, and red if it is due to lack of uplink power. The results from both figures are summarised in Table 5.7 in which the percentage of covered subscribers could be mapped to area coverage probability. Using D.O. Reudink's relation between edge coverage probability and area coverage probability [3] with a propagation exponent set to 3.52 as in Table 5.1 and a shadowing standard deviation set to 8.5dB, an ECP of 65% corresponds to and ACP of 84.1%. The result from SALTED scenario gives

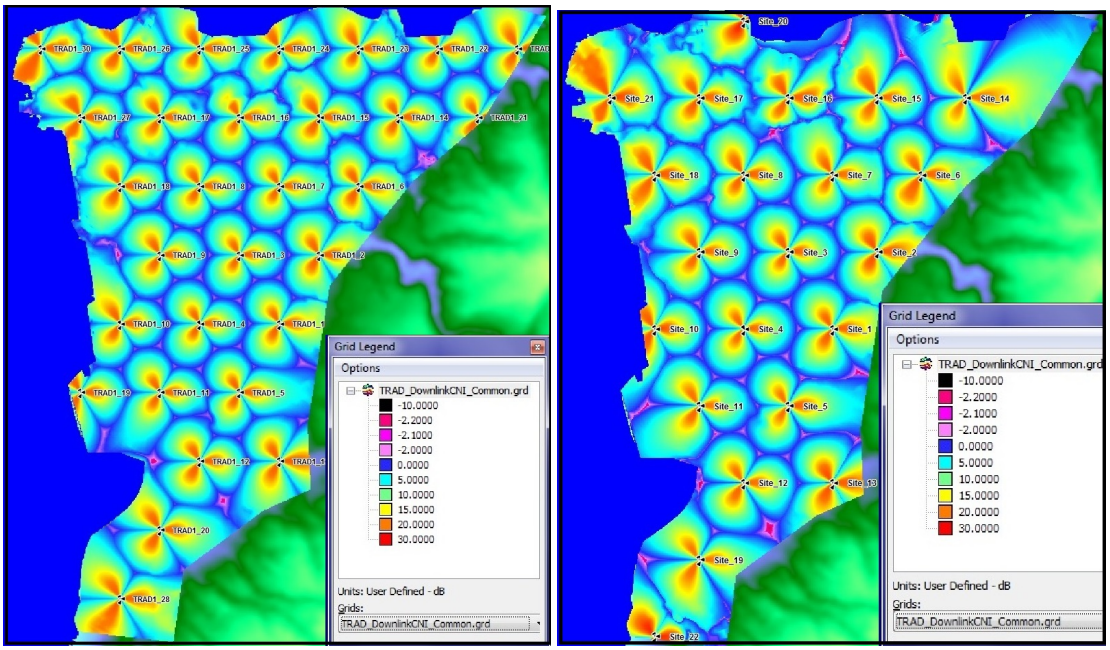

(a) Downlink SINR coverage plot in the traditional scenario.

(b) Downlink SINR coverage plot in the SALTED scenario.

Figure 5.3: Plots showing the SINR plots for both scenarios and indicating the site locations obtained through the ACP of Mentum Planet.

82.4% ACP which is very close to the target (ECP 65%) and the difference may be justified by the reduction in sites compared to results in Section 5.2. On the other hand, an ACP of 91.1% as obtained by the traditional scenario correspond to an ECP of 75% which exceed considerably the design target. Results from the traditional scenario show better performance since about 92% of the users have the required coverage performance.

Moreover, it is interesting to note that the average downlink cell load in the SALTED simulations case is 53.1% (Table 5.6) which is very close to 54.75% as calculated in SALTED (Table 5.4). Although this outcome on its own cannot be generalised is it however a good indication that capacity estimation in SALTED matches well simulations results in this case study.

Moreover, Mentum Planet generates a binary coverage plot that is positive if at least one MCS can be achieved in a given pixel and negative otherwise. Results from both scenarios are shown in Figures 5.6 (a) and (b) and are summarised in Table 5.8. The percentage of covered area shown maps directly to the area coverage probability but the results from Mentum Planet exceed the target in

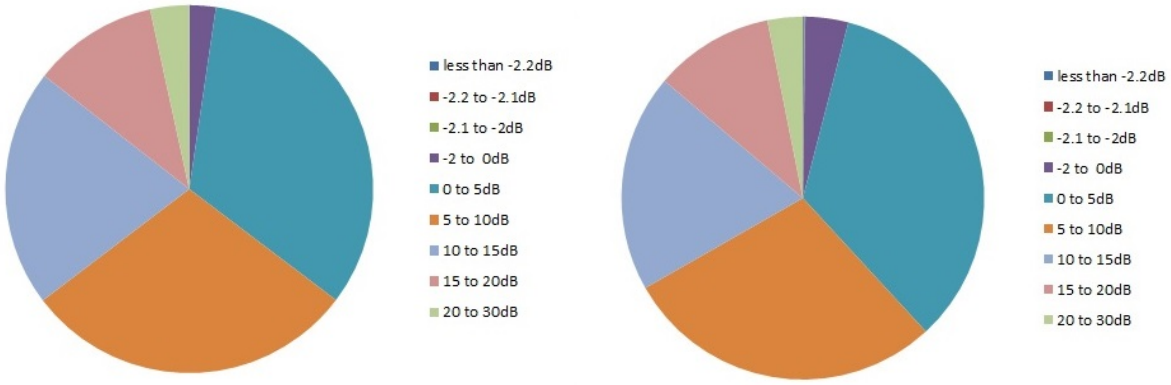

(a) DL SINR ranges for traditional scenario.

(b) DL SIN5 ranges for SALTED scenario.

Figure 5.4: DL SINR distribution for traditional and SALTED scenarios as obtained from Mentum Planet.

Table 5.6: Downlink cell load results from Mentum Planet.

Downlink cell load (%)	Traditional	SALTED
less than 30	17	8
between 30 and 40	20	5
between 40 and 50	34	12
more than 50	19	41
Average	40.85	53.1
Total number of sectors	90	66
Total number of sites	30	22

both scenarios. The downlink coverage plot as generated by Mentum Planet is based on the SINR value in the downlink as represented in Figure 5.4, thus it can be expected that the probability of coverage would be high. The extra dimension that is considered in the Monte Carlo results shown in Table 5.7 is the power pooling where DL power control is applied for each link to achieve the required SINR, thus subscribers that do not have coverage are dropped because of lack of power and not SINR value. This dynamic is not captured in dimensioning generally and in SALTED specifically. Thus the coverage plot gives an indication if a subscriber were to be in a given pixel would have the require SINR or not. Monte calro simulations give an indication that this subscriber in the same pixel, in the presence of all other subscriber in the network, would have the require SINR and the required DL power from the serving sector.

Realistically, monte carlo results are more representative of actual subscriber status, in which case SALTED provides a very good approximation. Even if

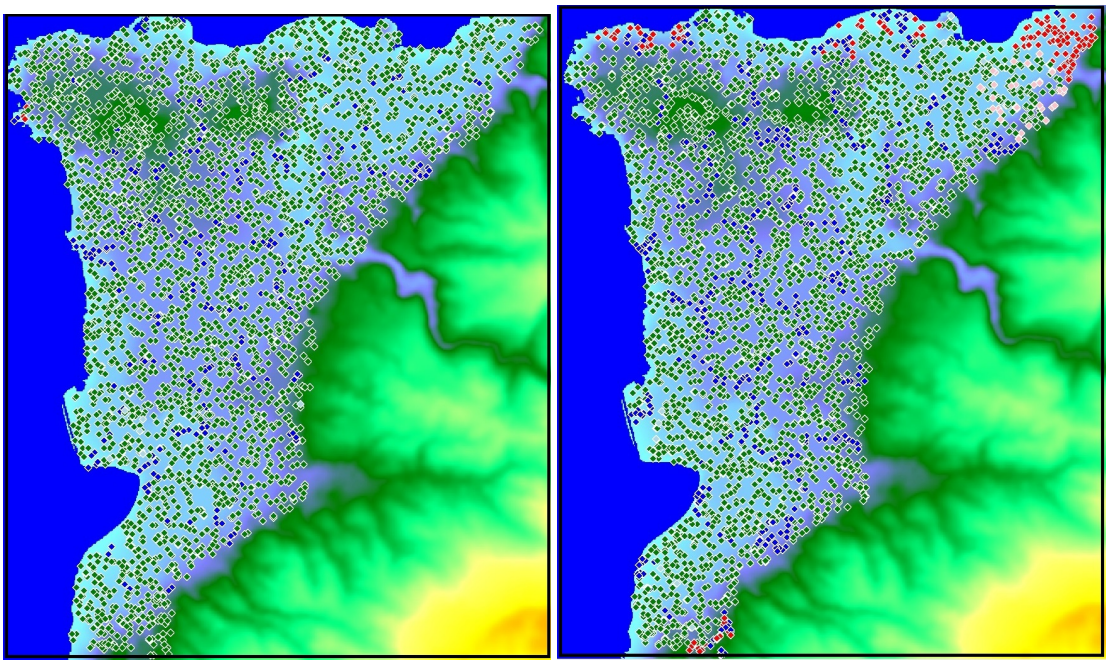

(a) Traditional scenario.

(b) SALTED scenario.

Figure 5.5: Monte carlo generate subscriber distribution in Ras Beirut using the traditional and SALTED scenarios. Subscribers are represented by a green diamond if they have coverage, blue if the they are out of coverage due to lack of downlink power, and red if it is due to lack of uplink power.

downlink coverage plots were to be considered the benchmark, SALTED gives better results compared to the traditional approach even if it may lead to over-dimensioning in some scenarios.

Table 5.7: Monte carlo simulation results.

Monte carlo results	Traditional	SALTED
Number of subscribers spread	3558	3576
Number of successes	3270	2945
Percentage success	91.1%	82.4%

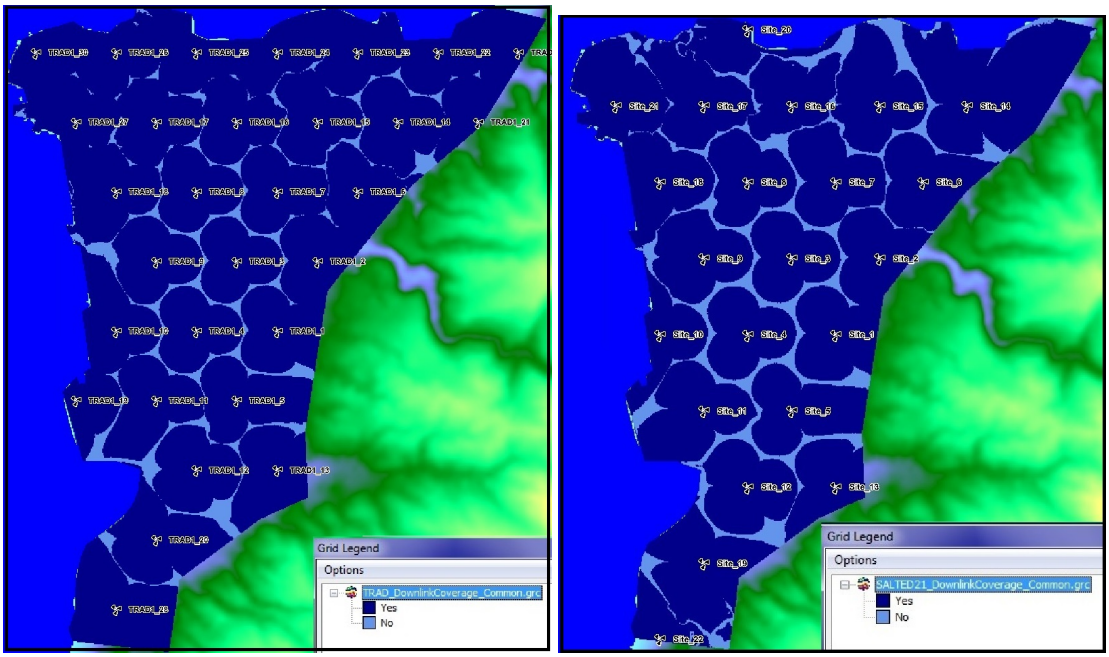

(a) Traditional scenario.

(b) SALTED scenario.

Figure 5.6: Downlink coverage plot in Ras Beirut using the traditional and SALTED scenarios.

Table 5.8: Downlink coverage results.

	Traditional	SALTED
Covered area (km^2)	62.4	59.7
Total area (km^2)	66.4	66.4
ACP	94.0%	89.9%

Chapter 6

Conclusion

In this thesis we were set to develop an LTE network radio dimensioning approach that is purely analytical but also dynamic to be able to capture the flexible features of the technology. An extensive literature review of state of the art LTE RND methodologies indicated three main line of research towards this end: re-adapting traditional link budget analysis; outage estimation based on statistical inter cell interference (ICI) analysis focused on a single sub-carrier; and a similar study assuming multi sub-carriers. The first RND group fails to capture the tight coupling between capacity an coverage and pragmatically accounts for channel variation effect. As is demonstrated in this work, the traditional approach often leads to over-dimensioning hence unjustified increase in both capital and operational expenditure. ICI based outage analysis assuming multi sub-carriers often required simulations, high computational load, and sometimes omits channel fading effect on interfering cells; thus in its current form it is not suitable for dimensioning purposes. ICI analysis based on single sub carrier as proposed in the literature is not comprehensive of all key dimensioning factors. Our proposed scheme is based on a single sub-carrier ICI analysis that takes into account, fading, shadowing on serving and interfering cells as well as cell loading (related to capacity) thus represents a comprehensive LTE RND methodology.

ICI statistical analysis is extended to define statistical distributions of key link budget entities namely: SINR, noise rise, maximum allowed path loss (MAPL) and cell range, all on the downlink direction. The approach is referred to as statistical link budget analysis (SLBA). Experimental results from these distributions indicated a close coupling between cell loading, which reflects the percentage or probability of user activity on the given subcarrier, and the resulting cell range. Two LTE dimensioning characteristics are revealed: cell breathing and cell elasticity. Cell breathing is the tradeoff between increased cell load, hence increased noise rise, then reduced MAPL and consequently smaller cell range and visa versa. The cell elasticity is another side-effect of cell load variation whereby higher cell load results in wider standard deviation of the cell range distribu-

tion thus more elasticity at the cell boundaries. Besides, the results show high sensitivity to inter-site distance definition; a 100 meters difference in inter-site distance is shown to degraded the network performance to unacceptable values.

Inspired by these results, SLBA is then integrated in an iterative process that finds the balance between coverage and capacity requirements on one hand and finds the best inter-site distance that give the require coverage probability with the target SINR. The algorithm is implemented in a user friendly tool, statistical analysis of LTE dimensioning (SALTED), to facilitate realisation of what/if scenarios and fully grasp the intrinsic characteristics of LTE dimensioning. A sensitivity analysis is conducted using SALTED that evaluates the effect of different key input parameters on the dimensioning results. We demonstrate that having more stringent requirements on coverage probability results in lower cell ranges, for instance. Also, reducing penetration loss or target SINR increases cell range to a point where the system becomes capacity limited in which case further reductions do not affect the cell range anymore. Increasing power per subcarrier also increases the cell range until the design becomes capacity limited after which point increased power is matched by increased attenuation.

A case study is developed in which the same set of parameters and design targets are used in the traditional LTE RND, in SALTED, and in Mentum Planet, a professional network planning tool. In this context inter-site distance obtained through the traditional approach is used to automate an LTE network plan in Mentum Planet without further optimisation. The same is done with SALTED-derived inter-site distance. Monte carlo simulations and network analysis are conducted in both cases and the results are compared to the design targets. As shown, the traditional approach results in over dimensioning of the network hence achieving network quality better than the target and realising coverage probability higher than required, at the cost of about 22% additional redundant sites. Inter-site distance as obtained from SALTED results in closer, but still higher key performance indicator (SINR) than the design target. However coverage probability results in this scenario match well the targets and moreover resulting cell loads from monte carlo simulations also match the value obtained from SALTED. The outcomes and analysis presented advocate the advantages of SALTED in LTE radio network dimensioning which has proved to surpass the traditional approach is providing reliable dimensioning output analytically without any need for simulations.

The work presented in this thesis represents a comprehensive dimensioning methodology for LTE looking at downlink considerations only. However a complete methodology should analyse the uplink as well and find the balance between uplink and downlink constraints. Unfortunately it was not possible to develop this part of dimensioning within the scope of the work presented. Nonetheless, the

path and procedure for developing the missing part is well established and would certainly be part of future work. Moreover, the statistical distributions presented here are derived under two channel fading scenarios: Rayleigh fading only, and composite fading. It was not possible to find a closed form distribution of the SINR assuming composite fading thus an approximation is suggested and validated. Further efforts will be put into finding a closed form for the SINR under composite fading since it was proved that the accuracy of SALTED results would be positively affected.
Accordingly, the future work can be summarised in the following research items:

1. Find closed form SINR distribution in case of composite fading and incorporated into SALTED.

2. Develop uplink SLBA for both Rayleigh and composite fading, incorporate into SLBA and SALTED.

3. Incorporate LTE-A advanced features within SALTED such as fractional frequency planning.

Appendix A

Abbreviations

3GPP	Third Generation Partnership Project
ACP	Area Coverage Probability
BER	Bit Error Rate
BS	Base Station
CDF	Cumulative Distribution Function
DL	Down Link
EbNo	Energy per Bit to Noise density ratio
ECP	Edge Coverage Probability
EESM	Exponential Effective SINR Mapping
EiRP	Effective Isotropic Radiated Power
FDMA	Frequency Division Multiple Access
FEC	Forward Error Correction
GSM	Global System for Mobile Communications
GUI	Graphical User Interface
ICI	Inter Cell Interference
LBA	Link Budget analysis
LTE	Long Term Evolution
MAPL	Maximum allowed path loss
MCS	Modulation and Coding Scehme
MGF	Moment Generating Function
MIC	Mean Instantaneous Capacity
OFDMA	Orthogonal Frequency Division Multiple Access
PA	Power Amplifier
PDF	Probability Probability Density Function
PHY	Physical
RB	Resource Block
RND	Radio Network Dimension
RNP	Radio Network Planning
SINR	Signal to Interference and Noise Ratio
SLBA	Statistical Link Budget analysis

SNR	Signal to Noise Ratio
TDMA	Time Division Multiple Access
UL	Up Link
UMTS	Universal Mobile Telecommunications System

Bibliography

[1] P. Bernardin, M. Yee, and T. Ellis, "Cell radius inaccuracy: a new measure of coverage reliability," *IEEE Transactions on Vehicular Technology*, vol. 47, no. 4, pp. 1215–1226, Nov 1998.

[2] A. Abdel Khalek, L. Al-Kanj, Z. Dawy, and G. Turkiyyah, "Optimization models and algorithms for joint uplink/downlink UMTS radio network planning with SIR-based power control," *IEEE Transactions on Vehicular Technology*, vol. 60, no. 4, pp. 1612–1625, May 2011.

[3] D. Reudink, *Microwave Mobile Communications*, ch. 2, pp. 126–128. IEEE Press, edited by Jakes, W.C. ed., 1993.

[4] M. Hata, "Empirical formula for propagation loss in land mobile radio services," *IEEE Transactions on Vehicular Technology*, vol. VT-29, no. 3, pp. 317–325, Aug 1980.

[5] A. Selian, "FROM GSM TO IMT-2000 - A COMPARATIVE ANALYSIS." [Online], Available: www.itu.int/osg/spu/ni/3G/casestudies/GSM-FINAL.doc, September 2001.

[6] K. Sipila, Z.-C. Honkasalo, J. Laiho-Steffens, and A. Wacker, "Estimation of capacity and required transmission power of WCDMA downlink based on a downlink pole equation," 2000.

[7] H. Holma and A. Toskala, *LTE for UMTS: Evolution to LTE-Advanced*. Wiley, 2nd ed., 2011.

[8] A. Fernekess, A. Klein, B. Wegmann, K. Dietrich, and M. Litzka, "Load dependent interference margin for link budget calculations of OFDMA networks," *IEEE Communications Letters*, vol. 12, no. 5, pp. 398–400, May 2008.

[9] A. B. Syed, "Dimensioning of LTE network, description of models and tool, coverage and capacity estimation of 3GPP long term evolution, radio interface," Master's thesis, Dept. Electrical and Communications Engineering, Helsinki University of Technology, Espoo, Finland, February 2009.

[10] A. Salo, M. Nur-Alam, and K. Chang, "Practical introduction to LTE radio planning." [Online], Available: http://digitus.itk.ppke.hu, November 2010.

[11] C. Seol and K. Cheun, "A statistical intercell interference model for downlink cellular OFDMA networks under log-normal shadowing and multipath Rayleigh fading," *IEEE Transactions on Communications*, vol. 57, no. 10, pp. 3069–3077, October 2009.

[12] C. Seol and K. Cheun, "A statistical intercell interference model for downlink cellular OFDMA networks under log-normal shadowing and multipath Ricean fading," *IEEE Communications Letters*, vol. 14, no. 11, pp. 1011–1013, November 2010.

[13] D. Ben Cheikh, J. M. Kelif, M. Coupechoux, and P. Goldewski, "SIR distribution analysis in cellular networks considering the joint impact of path-loss, shadowing and fast fading," *EURASIP Journal on Wireless Communications and Networking*, DOI:10.1186/1687-1499-2011-137, October 2011.

[14] X. Yang and A. Fapojuwo, "Coverage probability and spectral efficiency for downlink hexagonal cellular networks with Rayleigh fading," in *IEEE 24th International Symposium on PIMRC*, September 2013.

[15] H. Tabassum, F. Yilmaz, Z. Dawy, and M. S. Alouini, "A framework for uplink intercell interference modeling with channel-based scheduling," *IEEE Transactions on Wireless Communications*, vol. 12, no. 1, pp. 206–216, January 2013.

[16] WiMAX forum, "WiMAX system evaluation methodology." version 2.1, July 2008.

[17] R. Giuliano and F. Mazzenga, "Dimensioning of OFDM/OFDMA-based cellular networks using exponential effective SINR," *IEEE Transactions on Vehicular Technology*, vol. 58, no. 8, pp. 4204–4213, October 2009.

[18] Nortel Networks, "Effective SIR computation for OFDM system-level simulations," in *3GPP TSG RAN WG1 Meeting*, vol. 35, (Lisbon, Portugal), November 2003.

[19] J. Kelif, M. Coupechoux, and P. Godlewski, "On the dimensioning of cellular OFDMA networks," *Physical Communication*, vol. 5, no. 1, pp. 10–21, March 2012.

[20] S. Al-Ahmadi and H. Yanikomeroglu, "On the approximation of the generalized-K distribution by a gamma distribution for modeling composite fading channels," *IEEE Transactions on Wireless Communications*, vol. 9, no. 2, pp. 706–713, February 2010.

[21] Z. Dawy, S. Jaranakaran, and S. Sharafeddine, "Intercell interference margin for CDMA uplink radio network planning," in *15th IEEE International Symposium on PIMRC*, vol. 4, pp. 2840–2844, Sept 2004.

[22] InfoVista, "Mentum Planet." [Online], Available:http://www.infovista.com/products/Radio-Access-Network-planning-and-optimization.